NAVAL POSTGRADUATE SCHOOL
Monterey, California

AD-A257 859

DTIC
ELECTE
DEC 0 4 1992
S A D

THESIS

THERMOMECHANICAL PROCESSING OF
ALUMINUM ALLOY 2519 FOR GRAIN
REFINEMENT AND SUPERPLASTICITY

by

Scott D. Bohman

June, 1992

Thesis Advisor: T.R. McNelley
Co-Advisor: P. Kalu

92-30846

REPORT DOCUMENTATION PAGE

Form Approved
OMB No 0704-0188

1a REPORT SECURITY CLASSIFICATION Unclassified	1b RESTRICTIVE MARKINGS
2a SECURITY CLASSIFICATION AUTHORITY	3 DISTRIBUTION/AVAILABILITY OF REPORT Approved for public release; distribution is unlimited.
2b DECLASSIFICATION/DOWNGRADING SCHEDULE	

4 PERFORMING ORGANIZATION REPORT NUMBER(S)	5 MONITORING ORGANIZATION REPORT NUMBER(S)

6a NAME OF PERFORMING ORGANIZATION Naval Postgraduate School	6b OFFICE SYMBOL (If applicable) ME	7a NAME OF MONITORING ORGANIZATION Naval Postgraduate School
6c ADDRESS (City, State, and ZIP Code) Monterey, CA. 93943-5000		7b ADDRESS (City, State, and ZIP Code) Monterey, CA. 93943-5000

8a NAME OF FUNDING/SPONSORING ORGANIZATION	8b OFFICE SYMBOL (If applicable)	9 PROCUREMENT INSTRUMENT IDENTIFICATION NUMBER
8c ADDRESS (City, State, and ZIP Code)		10 SOURCE OF FUNDING NUMBERS

PROGRAM ELEMENT NO	PROJECT NO	TASK NO	WORK UNIT ACCESSION NO

11 TITLE (Include Security Classification)

Thermomechanical Processing of Aluminum Alloy 2519 for Grain Refinement and Super-Plasticity

12 PERSONAL AUTHOR(S)
Scott D. Bohman

13a TYPE OF REPORT Master's Thesis	13b TIME COVERED FROM _____ TO _____	14 DATE OF REPORT (Year, Month, Day) 1992 June 18	15 PAGE COUNT 89

16 SUPPLEMENTARY NOTATION

The views expressed in this thesis are those of the author and do not reflect the official policy or position of the Department of Defense or the U.S. Government.

17 COSATI CODES			18 SUBJECT TERMS (Continue on reverse if necessary and identify by block number)
FIELD	GROUP	SUB-GROUP	Aluminum-Copper Alloys, Superplasticity, Thermomechanical Processing

19 ABSTRACT (Continue on reverse if necessary and identify by block number)

Thermomechanical processing (TMP) methods developed for Al-Mg and Al-Mg-Li alloys have been modified and applied to the commercial 2519 Al-Cu alloy. The TMP included initial overaging and was designed to facilitate particle-stimulated nucleation (PSN) of recrystallization during controlled reheating intervals between successive rolling passes of the process. Effects of TMP variables were evaluated by tensile testing at temperatures ranging from 300-400°C. Strain rates varied from 6.7x10E-5 1/s to 6.7x10E-3 1/s. Also, microstructural analysis was conducted to determine the effect of the processing on the microstructure. The further evolution of microstructure during superplastic testing of the material was also assessed. Refinement to grain sizes below 10 microns by PSN was achieved. Superplastic ductility of 260 pct. elongation was limited by grain growth.

20 DISTRIBUTION/AVAILABILITY OF ABSTRACT ☒ UNCLASSIFIED/UNLIMITED ☐ SAME AS RPT ☐ DTIC USERS	21 ABSTRACT SECURITY CLASSIFICATION Unclassified
22a NAME OF RESPONSIBLE INDIVIDUAL Professor Terry R. McNelley	22b TELEPHONE (Include Area Code) (408) 646-2589	22c OFFICE SYMBOL MEMC

DD Form 1473, JUN 86   Previous editions are obsolete

S/N 0102-LF-014-6603

SECURITY CLASSIFICATION OF THIS PAGE
Unclassified

THERMOMECHANICAL PROCESSING OF ALUMINUM ALLOY 2519
FOR GRAIN REFINEMENT AND SUPERPLASTICITY

by

Scott D. Bohman
Lieutenant, United States Navy
B.S., Industrial Engineering, Oregon State University, 1986

Submitted in partial fulfillment
of the requirements for the degree of

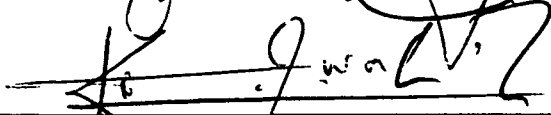## MASTER OF SCIENCE IN MECHANICAL ENGINEERING

from the

NAVAL POSTGRADUATE SCHOOL
June 1992

Author: _____

Scott D. Bohman

Approved by: _____

Terry R. McNelley, Thesis Advisor

_____

Peter N. Kalu, Co-Advisor

_____

Anthony J. Healy, Chairman
Department of Mechanical Engineering

ABSTRACT

Thermomechanical processing (TMP) methods developed for Al-Mg and Al-Mg-Li alloys have been modified and applied to the commercial 2519 Al-Cu alloy. The TMP included initial overaging and was designed to facilitate particle-stimulated nucleation (PSN) of recrystallization during controlled reheating intervals between successive rolling passes of the process. Effects of TMP variables were evaluated by tensile testing at temperatures ranging from 300-450°C. Strain rates varied from 6.7×10^{-5} s^{-1} to 6.7×10^{-3} s^{-1}. Also, microstructural analysis was conducted to determine the effect of the processing on the microstructure. The further evolution of microstructure during superplastic testing of the material was also assessed. Refinement to grain sizes below 10 μm by PSN was achieved. Superplastic ductility of 260 pct. was limited by grain growth.

iii

TABLE OF CONTENTS

LIST OF TABLES

LIST OF FIGURES

I. INTRODUCTION

The ability of some metallic materials to undergo large tensile elongations without localized necking is known as superplasticity. Tensile elongations in excess of 200 pct. are usually indicative of superplasticity, and elongations greater then 1000 pct. are not uncommon [Ref. 1]. Because of these high ductilities, superplasticity allows the designer to fabricate complex parts from one piece of metal in a single forming operation. Superplastic forming (SPF) reduces or eliminates the use of fasteners, reduces weight and decreases production time and cost while maintaining a high degree of dimensional accuracy. Eliminating the need for fasteners not only reduces weight but also reduces assembly, inspection and maintenance costs. Stress concentrations and the resulting susceptibility to fatigue and corrosion are also diminished. Conventional cold-formed parts may have significant residual stresses and thus tend to reshape themselves to their original unformed configuration. This is termed springback. Because of the high temperatures used, SPF parts have minimal residual stresses, thereby eliminating the need to compensate for springback.

These advantages over standard engineering materials and fabrication methods initially generated interest in the aerospace industry, but recently they have generated much interest for a number of commercial and other military application areas. Current applications of superplastic metals include landing gear doors for the B-1 bomber [Ref. 2], titanium and aluminum structures for the F/A-18A Hornet aircraft

1

[Ref. 3], and light weight coolant piping and fire control radar dishes [Ref. 4] to name just a few.

Most alloys are not inherently superplastic but can often be rendered superplastic by modifying the alloy composition and the thermomechanical processing (TMP) of the material. Superplasticity can be induced in many aluminum alloys by TMP. Two such processes widely used today are the Supral process and the Rockwell process. Both processes are designed to produce fine, equiaxed grains with high-angle grain boundaries and a uniformly dispersed second-phase precipitate to retard grain growth.

The Supral process is used for Al-Cu-Zr alloys and emphasizes continuous recrystallization (CRX) to obtain the requisite microstructure [Ref. 5]. The zirconium is added to form fine Al_3Zr particles that help retard grain growth following dynamic recrystallization during superplastic deformation (SPD) at 460°C [Ref. 6]. The Rockwell process was developed for aluminum alloy 7475 Al-Zn-Mg-Cu and employs overaging followed by cold working. The overaging produces second-phase particles that serve as nucleation sites for subsequent recrystallization at 482°C [Ref. 6].

Research at the Naval Postgraduate School, (NPS) has also been directed toward the study and development of superplastic aluminum alloys. Results of previous research has shown that the superplastic response is very sensitive to various TMP parameters and has led to a superplastic processing technique that achieves a significant superplastic response at lower temperatures than either the Supral process or the Rockwell process [Ref. 7]. This process has resulted in elongations in excess of 1000 pct. at 300°C

due to microstructural refinement via particle-stimulated nucleation (PSN) of recrystallization during TMP of an Al-Mg alloy [Ref. 8].

The ultimate goal of the current research is to apply previously developed processing techniques developed for the Al-Mg alloys to achieve a similar, low-temperature superplastic response (i.e., at $T \approx 300°C$) in a commercial Al-Cu alloy 2519. This goal will be approached by characterizing the microstructural evolution during TMP and determining the effects of this evolution on the superplastic response.

II. BACKGROUND

A. ALUMINUM ALLOYS

Aluminum alloys have extensive commercial uses especially in applications where weight is an important consideration. They have excellent mechanical properties, resist corrosion and can be machined easily. Aluminum alloys can be divided into two main groups, wrought and cast. Wrought and cast aluminum alloys can be further divided into two subgroups, heat treatable and non-heat treatable [Ref. 9]. Cast alloys are formed by pouring molten metal into molds or ingots. They are designated by a standard four-digit number with a decimal between the third and fourth digits (e.g. XXX.X). Wrought alloys are plasticly deformed and are designated by a standard four-digit number (e.g. XXXX). The first digit indicates the main alloying element. For Al-Cu 2519 the "2" identifies copper as the major alloying element. The second digit numerates the alloy modification. If the second digit is zero, it indicates the original alloy. The last two digits have no numerical significance, except to identify the different aluminum alloys in the group. The alloy designation is often followed by a temper designation that identifies how the alloy was heat treated, aged, strained, etc. [Ref. 9].

1. Strengthening Mechanisms

Metals deform by slip processes involving the motion of dislocations through a crystal lattice [Ref. 10]. Strengthening is achieved by impeding the motion of dislocations. Aluminum alloys can be strengthened by a variety of mechanisms. Careful control of one or more of these mechanisms is necessary to achieve the desired mechanical properties. A summary of the strengthening mechanisms applicable to aluminum alloys is provided below.

a. Strain Hardening

Strain or work hardening relies on the generation of dislocations during plastic deformation. Strength is achieved mainly by the interactions of dislocations among themselves. These interactions reduce dislocation mobility, raising the stress to continue dislocation motion [Ref. 11].

b. Solid Solution Strengthening

Aluminum readily dissolves many elements to form solid solutions. The presence of solute atoms as substitutionals or interstitials distorts the crystal lattice of the pure material. This results in a stress fields in the vicinity of the solutes which interfere with movement of dislocations. The degree of strengthening achieved by this mechanism is governed by the relative size difference between solute and aluminum atoms. Larger additions of alloying elements will contribute to the overall strengthening up until the point where the solubility limit is exceeded. When this occurs, an insoluble second-phase

forms and strengthening may then increase by another strengthening mechanism, dispersion strengthening.

c. *Precipitation Hardening*

Precipitation hardenable alloys possess a temperature-dependent solubility of alloying elements characterized by decreasing solubility with decreasing temperature [Ref. 12]. Precipitation or age hardening is accomplished by first solution heat treating at a temperature above the solvus of any alloy element present. The solution treatment continues until a homogeneous single-phase solid solution is produced. After solution treatment, the alloy is quenched, producing a supersaturated solid solution (SSS). This material is not in equilibrium and, in the case of Al-Cu alloys, precipitation takes place at room temperature, resulting in natural aging. Precipitation results in the formation of a finely dispersed second- phase. The crystal lattice is disrupted by the presence of this second-phase and strengthening is again produced by inhibiting the movement of dislocations.

2. Al-Cu 2519

Al-Cu 2519 is a heat treatable wrought aluminum alloy with properties similar those of low carbon steel. Applications include those that requiring high- strength, light-weight and weldable material. The binary aluminum-copper phase diagram is shown in Figure 2.1 [Ref. 13]. The Al-Cu alloy 2519 has a copper content exceeding the maximum solubility of copper (5.65 wt. pct.) at the eutectic temperature of 548°C;

therefore, complete copper solutioning cannot occur and the undissolved (Al_2Cu) phase will persist throughout subsequent processing and heat treatments.

In Al-Cu alloys a succession of precipitates develop from a rapidly-cooled supersaturated solid solution. Precipitates develop sequentially either with increased temperature or increased time at temperature [Ref. 14]. The stages of precipitate structures are identified by the following notation:

$$SSS \rightarrow GP\text{-}I \text{ zones} \rightarrow GP\text{-}II \text{ zones or } \Theta'' \rightarrow \Theta' \rightarrow \Theta \text{ } (Al_2Cu).$$

In the initial stages of the aging process, the random distribution of copper atoms changes to the form of disk-like planar aggregates called Guinier-Preston or GP zones. These thin precipitates on the {100} planes in the aluminum matrix. As aging continues, more copper atoms diffuse to the precipitates forming GP-II zones. These aggregates create coherency strain fields that impede dislocation motion. The formation of GP zones is accompanied by increased strength and decreased ductility [Ref. 15]. At higher temperatures, precipitates develop a greater degree of order and are called Θ'. In the alloy's highest strength condition Θ'' and Θ' are present and the alloy is in the peak aged condition. As time and/or temperature are further increased the stable, incoherent Θ precipitate is produced. As a larger portion of the Θ precipitates, the alloy softens and is said to be overaged.
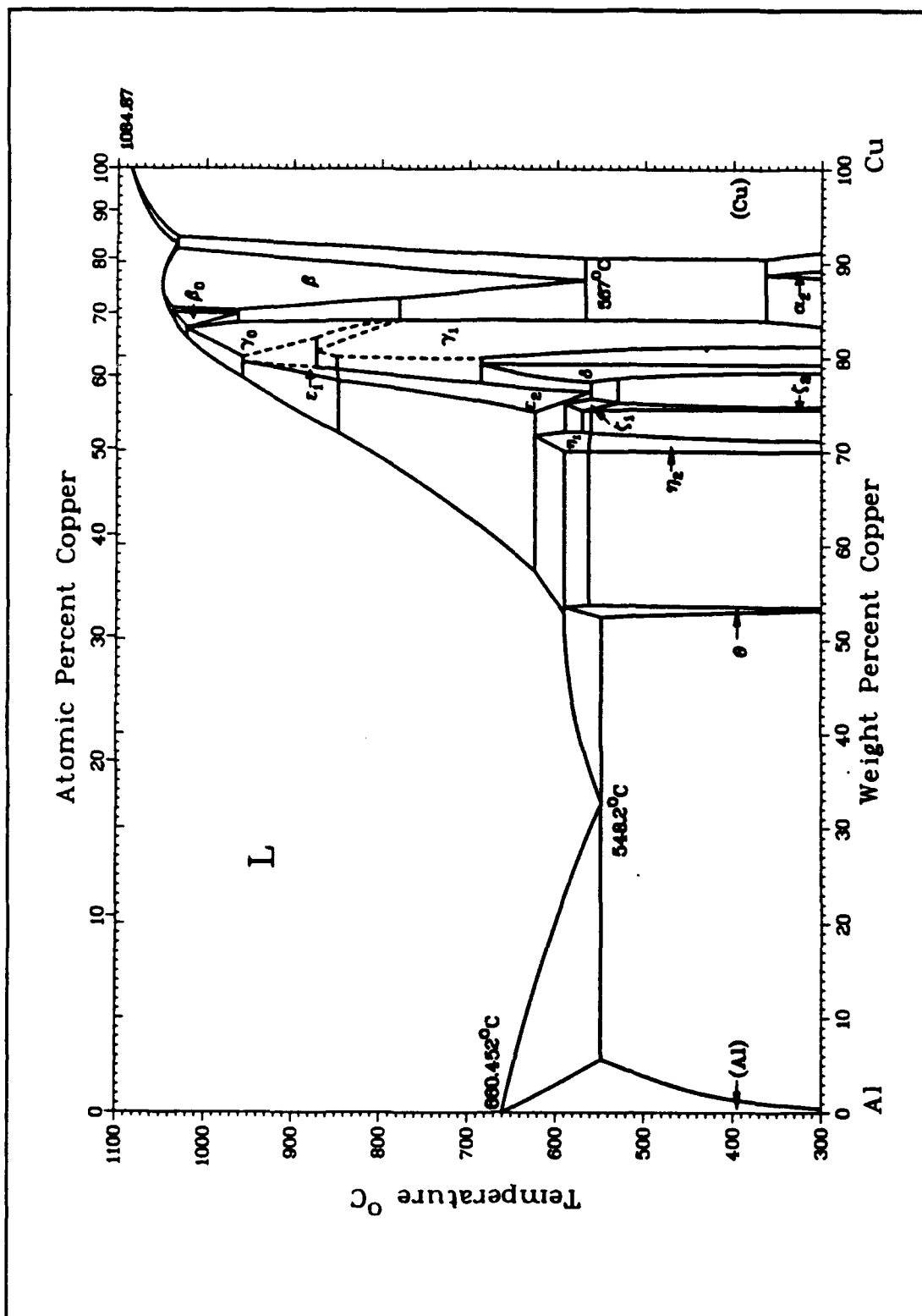
Figure 2.1. Al-Cu Phase Diagram [Ref. 13].

8

B. SUPERPLASTICITY

1. Microstructural Development

In order for a material to respond superplastically it must possess: (1), fine equiaxed grains, typically less than 10 μm in size; (2), a uniform distribution of second-phase particles to stabilize the grain structure; and (3), a large area fraction of high angle grain boundaries [Ref. 16]. There are several grain-refining methods available that will produce fine grains in various alloys. Two modes of grain refinement by recrystallization are termed either continuous recrystallization (CRX) or discontinuous recrystallization (DRX). Both modes are strongly influenced by the size and distribution of second-phase precipitate particles. Continuous recrystallization has been used for grain refinement in superplastic Supral Al-Cu-Zr alloys and consists of the development and coalescence of subgrain structures to form fine grains during elevated temperature deformation [Ref. 17]. Discontinuous recrystallization is the process by which new grains nucleate and grow and thus involves grain boundary migration. Precipitate particles are employed in the Rockwell process to initiate DRX. This is accomplished in a single recrystallization heat treatment following extensive deformation at 200°C. The particles are formed in an overaging treatment and characterization by TEM [Ref. 7] suggests their size to be 0.5-1.0 μm.

Nucleation may initiate within deformation zones adjacent to precipitate particles that are larger than a critical size in deformed particle-containing alloys. Deformation zones are regions in which a high dislocation density due to straining has

resulted in the formation of a fine, cellular or subgrain structure. These cells or subgrains are rotated with respect to the surrounding matrix. The particle size necessary for nucleation of recrystallization within these deformation zones varies inversely with strain and thus can be influenced by TMP. The notion of second-phase particles larger than a critical size acting as nucleation sites for recrystallization grains is called particle stimulated nucleation (PSN) [Ref. 18]. This work shows that PSN is most readily achieved at large particles ($\geq$ 1 μm in size), comparable to the particle sizes reported for the Rockwell process [Ref. 6].

The recrystallized grain size is inversely proportional to the number of particles participating in the PSN process. Processing that involves large strains will increase the number of nucleations sites, resulting in a finer grain size. Small strains during rolling will provide fewer nucleation sites, resulting in a coarser grain structure. Particles smaller than the critical size may inhibit recrystallization by reducing the mobility of dislocations, dislocation structures, and grain boundaries. These may also assist in controlling grain growth during deformation at elevated temperatures.

2. Mechanics of Superplastic Flow

The forming of superplastic materials is greatly influenced by strain rate and temperature. Superplastic alloys exhibit resistance to localized necking during deformation at elevated temperatures, typically 0.5-0.65 T_m, where T_m is the melting temperature. The flow stress is highly dependent on strain rate, as described by the equation:

$$\sigma = K\dot{\epsilon}^{m}. \qquad (2.1)$$

where σ is the flow, $\dot{\epsilon}$ is the strain rate, K is a material constant, and m is the strain rate sensitivity coefficient [Ref. 1]. The strain rate sensitivity coefficient is obtained from experimental data by applying the following relationship:

$$m = \frac{d(\ln \sigma)}{d(\ln \dot{\epsilon})} \qquad (2.2)$$

Values of m $\approx$ 0.5 are associated with highly superplastic response. During tensile deformation, the presence of a neck leads to a local increase in strain rate and, for alloys with high m values, to a large increase in the flow stress within the necked region. The neck thus undergoes strain rate hardening, preventing further necking. The value of m is influenced by the strain rate itself as well as the microstructure of the alloy. High m values are achieved by grain refinement obtained by thermomechanical processing [Ref. 1].

C. SUPERPLASTIC PROCESSING TECHNIQUES

1. Superplastic Processing

The two most common thermomechanical processes used for aluminum alloys are the Supral process and the Rockwell process. The Supral process is applied to Al-Cu-Zr alloys to which sufficient zirconium is added to form fine second-phase particles which later tend to inhibit grain growth during CRX. The Supral process is a four-step process starting with a solution treatment followed by warm rolling. Recrystallization is

11

prevented during warm rolling by precipitation of fine second-phase Al₃Zr particles and the absence of nucleation sites. After warm rolling, the material is cold worked to introduce sufficient strain energy prior to the last recrystallization step. Recrystallization (CRX) takes place during superplastic forming at the solution treatment temperature [Refs. 1,6].

The Rockwell process consists of: (1), a solution treatment; (2), overaging; (3), rolling at about 200°C; and (4), and a heat treatment resulting in DRX. The solution treatment is used to dissolve existing precipitate particles and produce a homogeneous single-phase solid solution. Then, overaging is employed to produce precipitate particles large enough to act as nucleation sites for recrystallization. In studies utilizing transmission electron microscopy, particles 0.5 to 1.0 μm in size were deemed sufficient for this purpose [Ref. 6]. Next, the alloy is rolled at 200°C to introduce dislocations structures essential for recrystallization. Finally, the alloy is heated and held at temperature long enough for recrystallization to occur. Rapid heating was shown to result in more highly refined grain structures compared to slower heating rates [Ref. 6].

2. Previous Research

Several studies at the Naval Postgraduate School (NPS) have led to the development of a TMP that produces a superplastic response in Al-10%Mg alloys at the relatively low temperature of 300°C. Additional studies have applied the TMP to a variety of alloys containing manganese or zirconium additions. The most recent TMP for Al-Mg alloys consists of a solution treatment and hot working (by upset forging) at the same temperature. After hot working, the material is quenched and then subsequently

12

warm rolled at 300°C. The warm rolling consists of a sequence of rolling passes with increasing strain and strain rate on successive passes and with controlled reheating between each successive rolling pass (see Table 2.1 of Ref. 7). Thirty-minute reheating intervals improved the superplastic ductility of an Al-10Mg-0.1Zr alloy compared to shorter times [Ref. 7]. Increasing the strain per pass for later rolling passes resulted in a more fully recrystallized microstructure following TMP for this same Al-10Mg-0.1Zr alloy. Recent studies employing the backscatter imaging mode in the scanning electron microscope (SEM) have indicated that the final stage of microstructural refinement occurs via PSN of recrystallization in association with relatively large Al_8Mg_5 β-phase particles about 2.0 μm in diameter. Such particles are considerably larger than those of the Rockwell processing method and are more consistent with the sizes reported as necessary in other studies of PSN [Ref. 18].

3. Processing Al-Cu 2519 For Superplasticity

The goal of the thermomechanical processing applied to this Al-Cu 2519 alloy is to produce the microstructural conditions necessary to obtain a superplastic response. Preliminary work toward accomplishing this goal was conducted at NPS by Mathé [Ref. 19]. Mathé concluded that rolling at T = 200°C to provide a pre-strain of 10 pct. prior to overaging at 450°C for 10 hours resulting in a uniformly- distributed Θ phase with particles of size $\approx$ 1-2 μm [Ref. 19]. Previous research concerning the Al-Mg system suggested that second-phase particles of this size are necessary to serve as nucleation sites for grains during recrystallization involving PSN [Ref. 8]. For this study, the overaged material was thermomechanically processed at 300, 350 and 400°C using

13

TABLE 2.1 Al-Mg ROLLING SCHEDULE

PASS	INITIAL THICKNESS (in)	CHANGE IN THICKNESS (in)	TRUE STRAIN (pct.)	STRAIN RATE (1/s)
1	1.00	0.10	10.0	0.893
2	0.90	0.11	12.2	1.045
3	0.79	0.11	13.9	1.196
5	0.570	0.11	19.3	1.680
6	0.460	0.11	23.9	2.104
7	0.350	0.085	24.3	2.435
8	0.265	0.07	26.4	2.931
9	0.195	0.055	28.2	3.547
10	0.140	0.040	28.6	4.219
11	0.100	0.030	30.0	5.130
12	0.070	0.023	32.9	6.464

a modified version of a TMP schedule developed at NPS for the Al-Mg system. The results of this initial step resulted in a maximum elongation of 205 pct., with no differences among the three TMP process temperatures.

In the second phase of this study, the overaging time was increased from 10 hours to 50 hours and TMP was conducted at 300°C only. By increasing the overaging time, precipitate particles have more time to coarsen resulting larger particles, i.e., a higher volume fraction of particles of size $\approx$ 1-2 μm.

Phase three consisted of altering the TMP by using only five minute reheating intervals between rolling passes one through six and 30 minute reheats for passes seven

through nine. This modification was an attempt to increase the dislocation density and stored strain energy in the early part of the rolling process, while allowing sufficient time for recovery and possible PSN later in the process.

The final phase consisted of an anneal a higher temperature prior to tensile testing at a lower temperature. This modification was an attempt to determine the effect of producing a more fully recrystallized microstructure prior to tensile testing at lower temperatures. During each phase of the experiment microstructural analysis was conducted in an attempt to determine the effect of each modification to the TMP.

III. EXPERIMENTAL PROCEDURE

A. MATERIAL

The aluminum alloy 2519-T87 studied in this research was provided by the ALCOA Technical Center, ALCOA Center, Pennsylvania. The as-received material was supplied in the form of a rolled plate with dimensions 24 x 12 x 0.875 in. (609.6 x 304.8 x 22.2 mm) heat treated to a T87 temper condition (i.e. solutionized at 535°C, cold rolled to 7 pct. strain and artificially aged for 24 hours at 165°C [Ref. 20]).

The composition for the as-received alloy 2519 is provided in Table 3.1. Values listed are within the composition limits for 2519 specified in the Metals Handbook [Ref. 9].

TABLE 3.1 COMPOSITION OF AL-2519 (WEIGHT PERCENT)

Cu	Mn	Mg	Fe	Zr	V	Si	Ti	Zn	Ni	Be	B	Al
6.06	0.30	0.21	0.16	0.13	0.04	0.07	0.06	0.03	0.01	0.002	0.001	bal.

The as-received plate was sectioned into billets measuring 2.4 x 1.5 x 0.875 in. (61.0 x 38.1 x 22.2 mm). The billets were cut with the greatest dimension parallel to the rolling direction of the as-received plate.

B. PROCESSING

Billets were thermomechanically processed using a modified version of schedules originally developed at NPS for superplastic processing of Al-Mg alloys. The modified process employs a four step procedure consisting of: (1), solution treatment; (2), pre-strain; (3), overaging; and (4), rolling with controlled reheating between passes. Figure 3.1 is a schematic illustration of the essential elements of the TMP.

1. Solution Treatment and Pre-strain

The solution treatment process was designed to produce a uniform starting condition by dissolving the soluble components to produce a homogeneous solid solution. The solution treatment was performed in a Lindberg Furnace, Model 51828, by heating at 535°C for 100 minutes followed by a room-temperature water quench. A pre-strain of 10 pct. was then introduced to provide sufficient dislocations to serve as nucleation sites for the Θ phase (Al_2Cu) precipitates during subsequent overaging treatments. The billets were preheated to 200°C and warm rolled to a 10 pct. reduction using two passes of 5 pct. each. This procedure was adopted due to severe surface cracking and alligatoring (splitting of the ends) encountered during initial attempts to roll with a single at 10 pct. reduction. This cracking was determined to be associated with the particular rolling geometry (mill gap, billet thickness and reduction) used here and not with the particular material supplied.
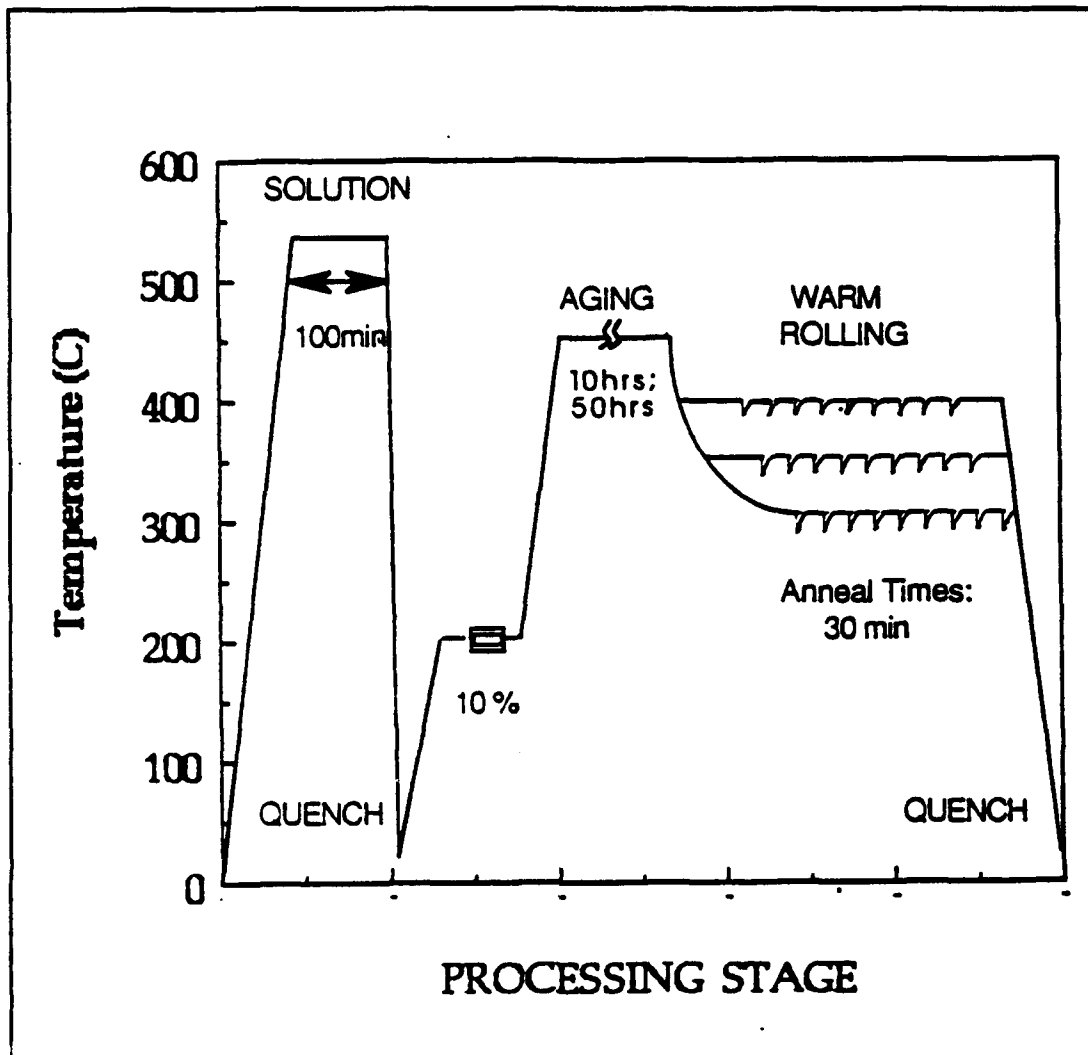
Figure 3.1. TMP Schematic Diagram.

2. Overaging

Billets were then overaged at 450°C for either 10 or 50 hours. Selection of the overaging times and temperature were based on previous research that attempted to achieve the microstructures similar to those of the Al-Mg system [Ref. 19]. The goal of the overaging process was to produce a uniform distribution of 1-2 μm precipitate particles that would serve as nucleation sites for recrystallized grains during subsequent

18

processing. After overaging, the billets were furnace cooled to the rolling temperature at a rate of no more than five degrees per hour.

3. Warm Rolling

The overaged billets were preheated to the rolling temperature and held there for 30 minutes prior to rolling. During the rolling process, billets were reheated during rolling passes for either 5 or 30 minutes depending on the TMP. All processes consisted of nine passes of increasing strain and strain rate on each successive pass. After completing the final pass, the rolled material was water quenched at room temperature. Samples were then sectioned from the end of the rolled for subsequent annealing and microstructural analysis of the as-rolled material. Rolling was conducted on a Fenn Laboratory rolling mill with roll diameters of 4.0 inches rotating at 0.327 radian/sec. Strains and strain rates for each pass were calculated using equations 3.1 and 3.2 respectively:

$$\epsilon_{pass} = \frac{t_i - t_f}{t_i} = \frac{\Delta t}{t_i} \, , \tag{3.1}$$

where ϵ_{pass} is the strain, t_i is initial thickness prior to the pass, and t_f is the final thickness after the pass, and:

$$\dot{\epsilon} = \frac{2\pi R n}{\sqrt{Rt_i}} \sqrt{\epsilon}(1 + \epsilon/4) \, , \tag{3.2}$$

where $\dot{\varepsilon}_{pass}$ is the strain rate, R is the radius of rolls (inches), and n is the rotational speed of rolls (rad/sec). Table 3.2 is an example of the rolling schedule followed for all processes.

TABLE 3.2 TMP ROLLING SCHEDULE

PASS	INITIAL THICKNESS (in)	MILL GAP SETTING (in)	FINAL THICKNESS (in)	MILL DEFLECTION (in)	TRUE STRAIN (pct.)	STRAIN RATE (1/s)
1	0.812	0.742	0.763	0.210	6.0	0.80
2	0.763	0.657	0.683	0.0255	9.9	1.07
3	0.683	0.581	0.603	0.220	11.6	1.27
4	0.603	0.513	0.538	0.245	10.9	1.27
5	0.538	0.431	0.456	0.245	15.3	1.61
6	0.456	0.338	0.363	0.246	20.4	2.04
7	0.363	0.227	0.259	0.320	28.5	2.76
8	0.259	0.123	0.163	0.040	37.1	3.80
9	0.163	0.045	0.078	0.034	51.8	5.85

C.   TENSILE TESTING

Upon completion of the warm rolling process, final sheet thicknesses were approximately 2.0 mm. Tensile test specimens were machined from the sheet, maintaining the rolling direction of the as-received plate as the longitudinal direction of the sample, to the dimensions given in Figure 3.2.
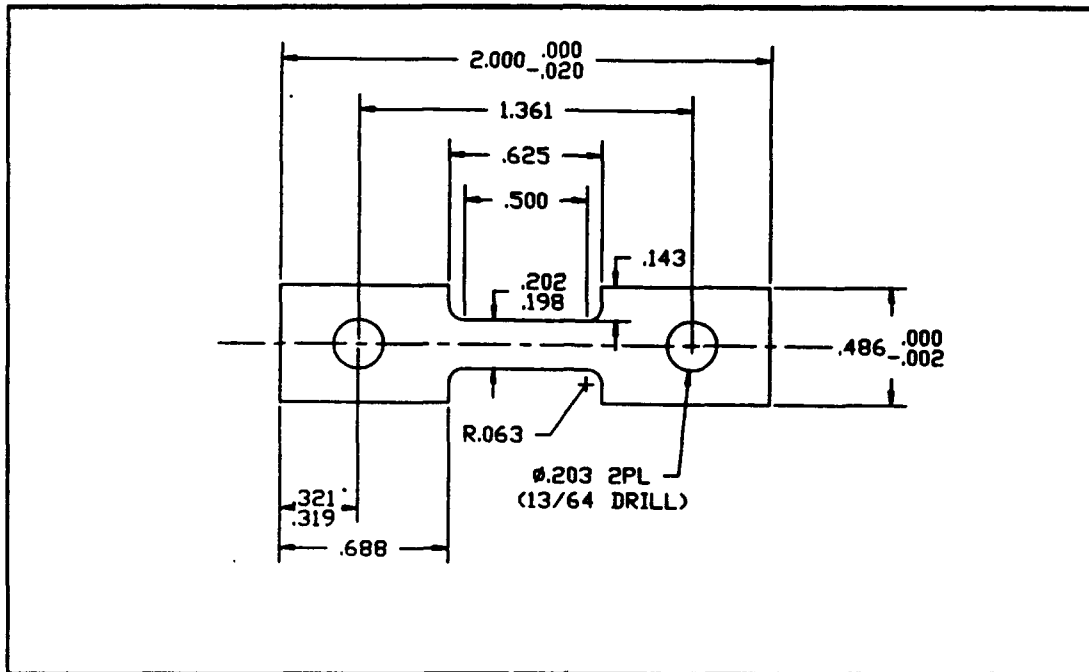
Figure 3.2. Tensile Test Specimen Drawing.

Tensile testing was conducted on an Instron Model 6027 test machine equipped with a 10 KN capacity load cell. A Marshall Model 2232 three zone clamshell furnace mounted on the test apparatus was used to maintain constant elevated temperatures during testing at temperatures of 300, 350, 400 and 450°C. A uniform temperature distribution within the furnace was monitored by eight type K thermocouples positioned approximately every two inches along the center line of the test apparatus. Temperature control was maintained by three independent Omega Model 49 proportioning controllers with one controller for each zone of the furnace. The samples were place in preheated grips (150°C) and given approximately 35 minutes in the clamshell furnace to equilibrate to test temperature. A summary of the tensile testing performed is given in Table 3.3.

21

TABLE 3.3 PROCESS CONDITION AND TEST TEMPERATURE MATRIX

Tensile Test Temperature (°C)	Rolling Temperature with Aging Time and Post Roll Annealing Time/Temperature						
	300°C 10hrs.	350°C 10hrs.	400°C 10hrs.	300°C 50hrs.	*300°C 50hrs.	*300°C 50hrs. 7min/400°C	*300°C 50hrs. 7min/450°C
300	X	X	X	X	X	X	X
350	X	X	X	X	X	X	X
400	X	X	X	X	X		X
450	X	X	X	X	X		

* note: 5 min. reheat time for passes 1-6 and 30 min. reheat time for passes 7-9.

Crosshead speeds corresponding to engineering strain rates of 6.67×10^{-5} s^{-1}, 6.67×10^{-4} s^{-1} and 6.67×10^{-3} s^{-1} were used. The resultant load versus displacement plots provided by the Instron testing apparatus were corrected to account for the elastic response of the test apparatus and tightening of the grips. The corrected data was then used to calculate true stress (σ) and true strain (ϵ). Graphs of σ versus ϵ are collected in Appendix A. The stress-strain plots were then used to obtain log true stress at a pre-determined strain versus strain rate data for an analysis of the strain-rate dependence of the stress. From the slope of the log σ versus log $\dot{\epsilon}$ plots, strain rate sensitivity coefficient, m, values were determined. A summary of m-values are found in Appendix B.

D. METALLOGRAPHY

1. Optical Microscopy

Optical microscopy was carried out to study the microstructural effects of the thermomechanical processing, in particular the effects of process parameters on grain size and precipitate size and distribution. Specimens were prepared at each step in the process including the grip and gage sections of various samples tested on the Instron.

Specimens were cold mounted in an acrylic compound, ground flat and polished following the procedure listed in Table 3.4. After polishing, the specimens were anodized in Barker's solution at room temperature for approximately 90 seconds. A constant voltage source operating at 18 VDC provided a current of in the range of 0.05-0.2 amperes. Metallographic examination was conducted with a Zeiss Photomicroscope III utilizing crossed polarizers to reveal grain contrast.

TABLE 3.4 SPECIMEN POLISHING SCHEDULE

Step	Polishing Medium	Time (min.)	Wheel RPM	Comments
1	240 Grit	3	N/A	Rotate 90°
2	600 Grit	3	N/A	Rotate 90°
3	3 Micron Diamond Paste	3-5	200-250	Counter-rotate Light pressure
4	1 Micron Diamond Spray	5-10	200-250	Counter-rotate Light pressure
5	Colloidal Silica	3-5	200-250	Counter-rotate

23

2. Scanning Electron Microscopy

Scanning electron microscopy was used to characterize the effect of process parameters on precipitate particle size and distribution. Specimens were mechanically polished using the same technique as that used for optical microscopy (see Table 3.4). The specimens were then electropolished using a solution of 90 pct. butoxyethenol and 10 pct. hydrochloric acid maintained at 0°C in a methanol bath cooled with liquid nitrogen. A constant 16 VDC potential supplied a current of approximately 0.04 amperes for three minutes, holding the specimens tangent to the outer edge of the vortex created by a magnetic stirrer. After electropolishing, the specimens were mounted with conducting paint and examined with scanning electron microscope (SEM). The SEM was operated in the backscatter mode with an accelerating voltage of 20 kV utilizing a LaB_6 filament.

IV. RESULTS AND DISCUSSION

This chapter will examine the effects on the microstructural development and mechanical behavior of the Al-Cu alloy 2519 considered in this study. Recent research on Al-Cu 2519 [Ref. 19] demonstrated that introducing a 10 pct. pre-strain prior to overaging at 450°C resulted in a more uniform distribution of nearly equiaxed second-phase precipitate particles. Aging for times varying from 10 to 50 hours resulted in particles of maximum size in the range of 1-3 μm [Ref. 19]. Particles of this size have been associated with PSN of recrystallization during TMP of Al-Mg alloys [Ref. 8]. The thermomechanical processing variables selected for investigation in this research consisted of the prior aging time; the rolling temperature; reheating times during rolling; and the post-roll annealing temperature. These factors were varied in such a manner to allow assessment of their effect on recrystallization during and after the TMP. Table 4.1 provides a complete summary of the processes. Ductility data for each TMP is summarized in Appendix C.

Optical and SEM microscopy was used to characterize the microstructural evolution of the differing TMP's and during subsequent tensile testing. Tensile testing at elevated temperatures was conducted to investigate deformation characteristics of materials processed by TMPs A-G. Test temperatures ranged from 300 to 450°C while strain rates ranged from 6.67 x 10^{-5} s^{-1} to 6.67 x 10^{-3} s^{-1}.

TABLE 4.1 TMP PROCESS SUMMARY

TMP	TMP PARAMETERS			
	PRE-ROLLING	ROLLING		POST ROLLING
	OVERAGING TIME (HRS)	TEMP (°C)	REHEATING TIME (MIN)	REXTAL TEMP/TIME
A	10	300	30	-
B	10	350	30	-
C	10	400	30	-
D	50	300	30	-
E	50	300	5	-
F	50	300	5/30	400°C/7 min
G	50	300	5/30	450°C/7 min

* note: 5 min. reheat time for passes 1-6 and 30 min. reheat time for passes 7-9.

A. MICROSTRUCTURAL CONDITION PRIOR TO ROLLING

SEM and optical micrographs were prepared from material which had been solution treated for 100 minutes at 535°C, pre-strained by 10 pct. at 200°C, and then overaged at 450°C for 10 hours. The choice of this overaging process was based on Mathé's results on particle size and distribution using SEM in the backscatter imaging mode. Figure 4.1 (a) is a typical SEM micrograph revealing white θ-phase precipitates in a dark alpha-phase matrix. This material had been overaged for 10 hours at 450°C. The θ-phase particles are light in contrast due to the high atomic number of copper compared to aluminum. The scattering efficiency of atoms increases as the atomic number

26

increases and more electrons will be deflected to the backscatter detector, resulting in a brighter image. The SEM backscattered imaging mode allows examination of the bulk structure and enables characterization of a full range of particle sizes. This method is well-suited for microstructure such as these and avoids possible selective thinning artifacts of thin-foil methods.

The Al-Cu 2519 alloy possesses a relatively high copper content (6.06 wt. pct.), and only small amounts of other elements such as magnesium (0.21 wt. pct.) and manganese (0.30 wt. pct.). Vietz and Polmear have shown that when the ratio of copper to magnesium concentrations in aluminum exceeds 8 to 1, Θ (Al$_2$Cu) is the primary precipitate [Ref. 21]. The Al-Cu 2519 alloy has a copper to magnesium ratio exceeding 28 to 1, and so the precipitates in Al-Cu 2519 will be the Θ phase. Contrast variations due to orientation differences in the matrix were not detected in SEM micrographs. Particles appear to be randomly distributed with the largest particles of size on the order of 1 to 2 μm.

Figure 4.1 (b) is a typical polarized-light optical micrograph of this material (overaged for 10 hours). The micrograph reveals a coarse-grain microstructure with grains on the order of 300-400 μm. Grains also tended to be aligned parallel to the rolling direction of the as-received plate. Comparisons between Figures 4.1 (a) and (b) can only be made after careful consideration of the large difference in magnification between the two micrographs. Precipitates are both inter-granular and intra-granular, with large precipitates forming stringers that are aligned parallel to the rolling direction of the as-received plate. These large precipitates probably were not completely dissolved during

27

solutioning, due to the high copper content, and formed bands during the rolling in original manufacture. They may also have coarsened during the prolonged overaging process.

B.   EFFECTS OF ROLLING ON THE MICROSTRUCTURE

Immediately after overaging, the material was processed using the thermomechanical technique described in Chapter III and summarized in Table 4.1. Initial work considered the effect of rolling temperature. Figure 4.2 (a) is a typical SEM micrograph revealing Θ-phase particle size and distribution upon completion of processing according to TMP A. The Θ phase particles appear to be uniformly-distributed, with a larger percentage of particles now exceeding 1.0 μm as compared to Figure 4.1 (a). The TMP appears to have promoted continued precipitation and coarsening of the smaller particles (Figure 4.1 (a)) while maintaining a uniform distribution.

(a)
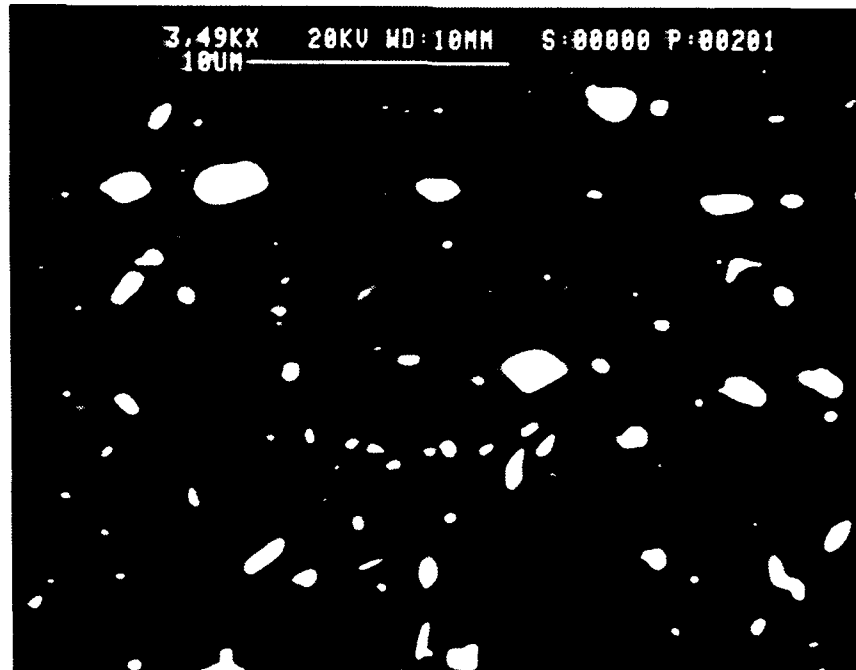
(b)

Figure 4.1 Al-Cu 2519 Alloy, After Overaging for 10 hours at 450°C. (a) SEM
Backscattered Micrograph; (b) Optical Micrograph (x105).

Optical micrographs show the typical microstructure of the as-rolled (Figure 4.2 (b)), and the rolled and annealed (Figure 4.2 (c)), materials. The overaged, coarse-grained microstructure shown in figure 4.1 (b), has been heavily deformed and elongated by the rolling process (see Figure 4.2 (b)). A careful comparison between these two micrographs shows that the grain thickness of the rolled material has been reduced by a factor of about ten. However, the grains are elongated by a lesser proportion, indicating that some refinement has taken place during the rolling itself. The precipitates appear to be similar in size and the banded appearance observed in Figure 4.1 (b) has been eliminated.

Subsequent annealing at 450°C for five minutes reveals an equiaxed fine-grain microstructure with an average grain size of approximately 11.1 μm (see Figure 4.2 (c)). The micrograph of the annealed material represents the material prior to tensile testing at 450°C. Microstructural examination of the as-rolled material annealed at temperatures of 300 and 350°C did not show such evidence of recrystallization. Instead, the microstructure appeared to retain elongated grains, suggesting only recovery processes occur during such short anneals at these lower temperatures. At the higher annealing temperatures of 400 and 450°C, recrystallized grains became evident and, at 450°C, the microstructure appeared to be fully recrystallized.
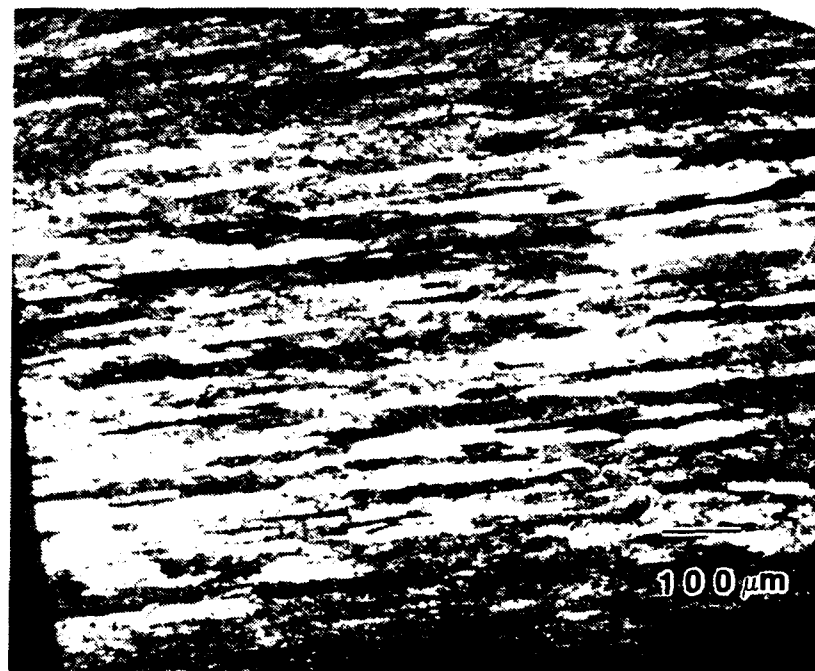
(a)

(b)

Figure 4.2   Al-Cu 2519 Alloy, After Rolling, TMP A. (a) SEM Backscattered Micrograph; (b) Optical Micrograph (x105); (continued);
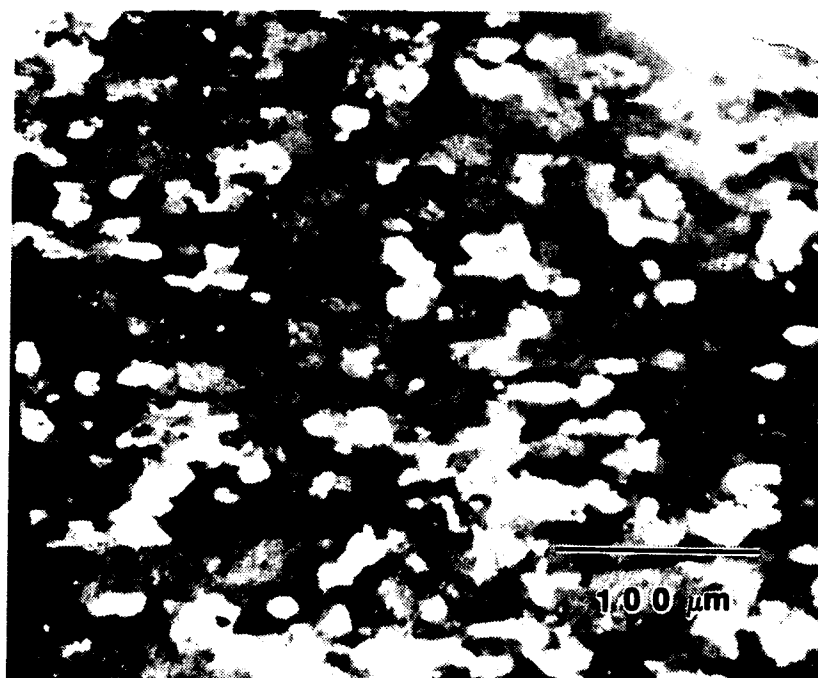
31

(c)

100 μm

Figure 4.2 (c) Optical Micrograph (x261), 5 min., Post TMP D Anneal at 450°C.

C.   EFFECTS OF THERMOMECHANICAL PROCESSING VARIABLES

1.   Rolling Temperature Effects

Figure 4.3 shows percentage elongation versus test temperature for materials processed according to TMP's A, B, and C. Testing was conducted at a constant strain rate of 6.67×10^{-4} s^{-1}. All three of the TMPs appear to be following the same general trend of gradual ductility increase with no consistent differences due to prior processing as test temperature increases over the interval from 300 to 450°C. Figure 4.4 plots true stress at 10 pct. true strain versus test temperature for specimens processed by TMPs A, B, and C.

Optical micrographs of the grip sections of specimens processed according to TMPs A, B, and C, and subsequently tensile tested at 450°C are shown in Figures 4.5 (a), (b), and (c), respectively. In all three cases, warm rolling with reheating intervals of 30 minutes between rolling passes produced a refined microstructure. Recrystallized grains maintained an alignment parallel to the rolling direction of the as-received plate. Precipitates are uniformly distributed, more equiaxed, and there are none of the deformation bands apparent prior to rolling (Figure 4.1 (b)). Grain sizes for TMPs A, B, and C measured 18.7, 19.3, and 19.1 μm, respectively. Optical micrographs and grain size measurements reveal no significant differences in grain size or microstructure as a function of the prior rolling temperature. The grain size obtained from these grip sections is coarser than that of the annealed sample of Figure 4.2 (c) due to more prolonged heating. The mechanical property data are also very similar and suggest only minimal
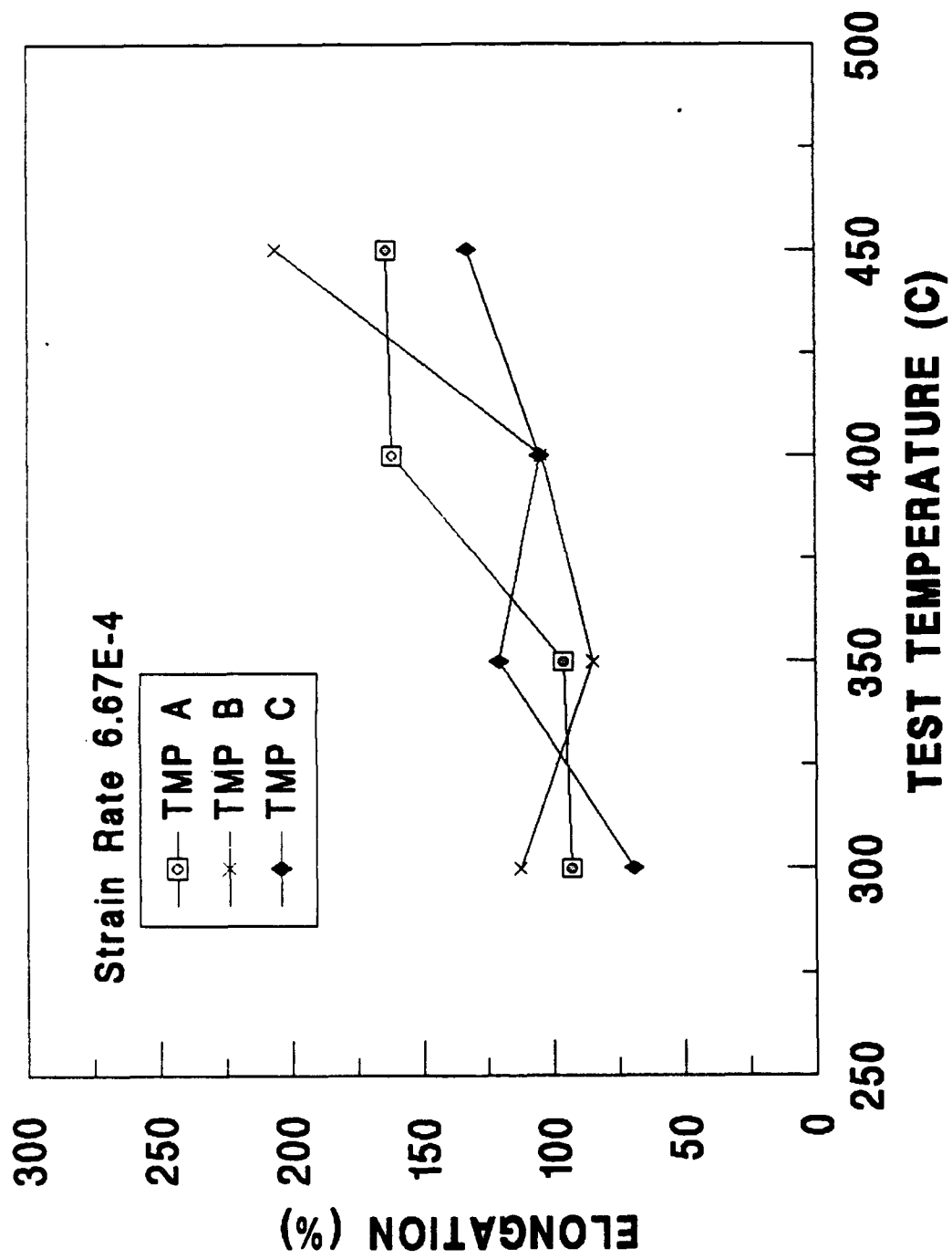
33

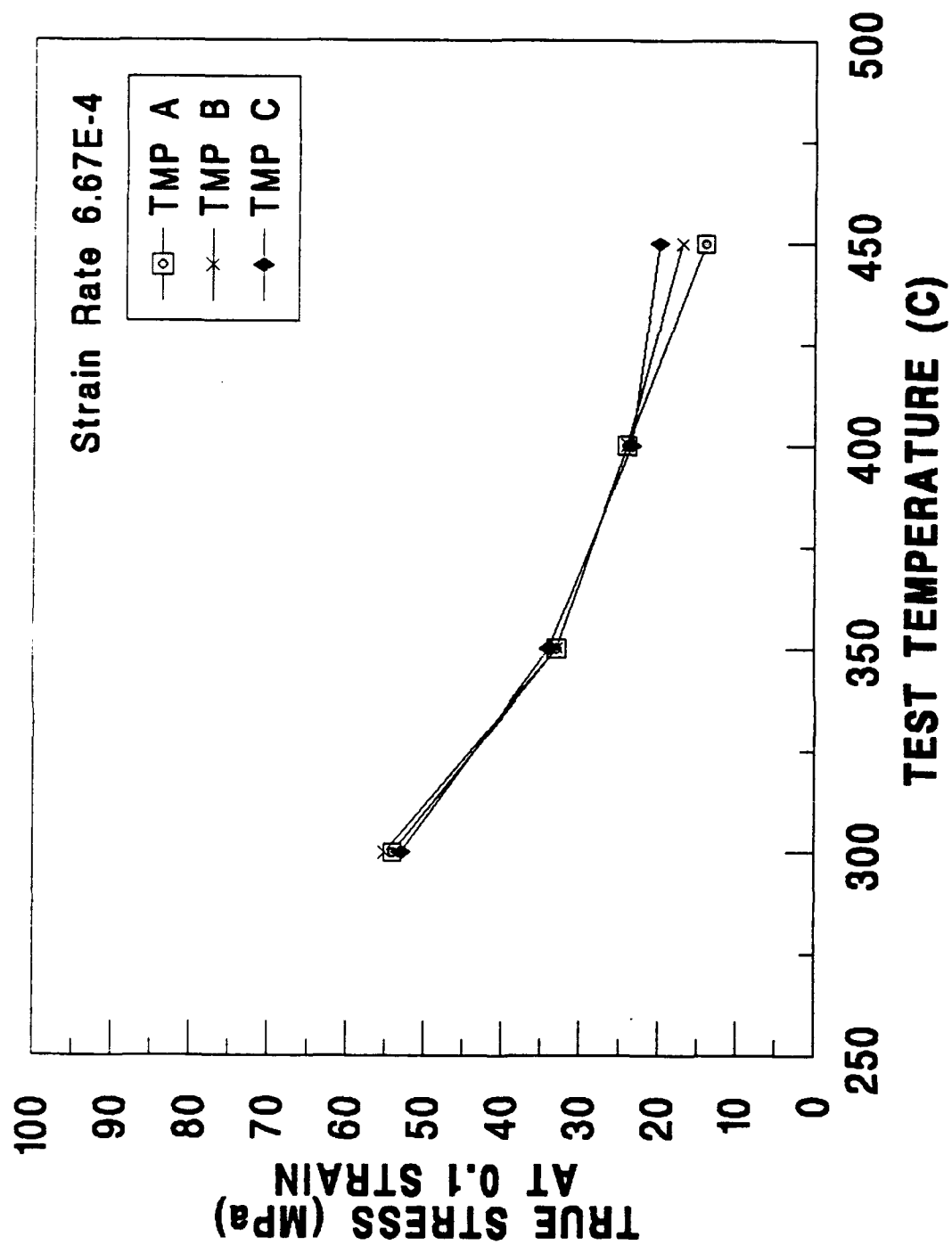Figure 4.3 Ductility vs. Test Temperature, TMPs A, B and C.

34

Figure 4.4 True Stress at 0.1 Strain vs. Test Temperature, TMPs A, B and C.

superplastic response (> 200 pct. elongation) at the highest temperature in this interval. Thus, varying the rolling temperature in the interval 300 to 400°C does not produce an appreciable effect on the recrystallized grain size or the mechanical properties of this material.

2. Aging Time Effects

The purpose of the overaging was to provide large precipitate particles capable of serving as nucleation sites for recrystallization either during the TMP itself or upon subsequent heat treatment. A higher volume fraction of precipitate particles exceeding a critical size will provide more such sites and thus refine the resulting grain structure [Ref. 18]. TMP A was modified by increasing the overaging time from 10 hours to 50 hours (TMP D). A more refined grain size and an increase in ductility was anticipated. The tensile test results for materials following TMP A and TMP D are contrasted in Figures 4.6 and 4.7. The increased overaging time results in a softer, weaker material at all test temperatures as well as enhanced ductility.
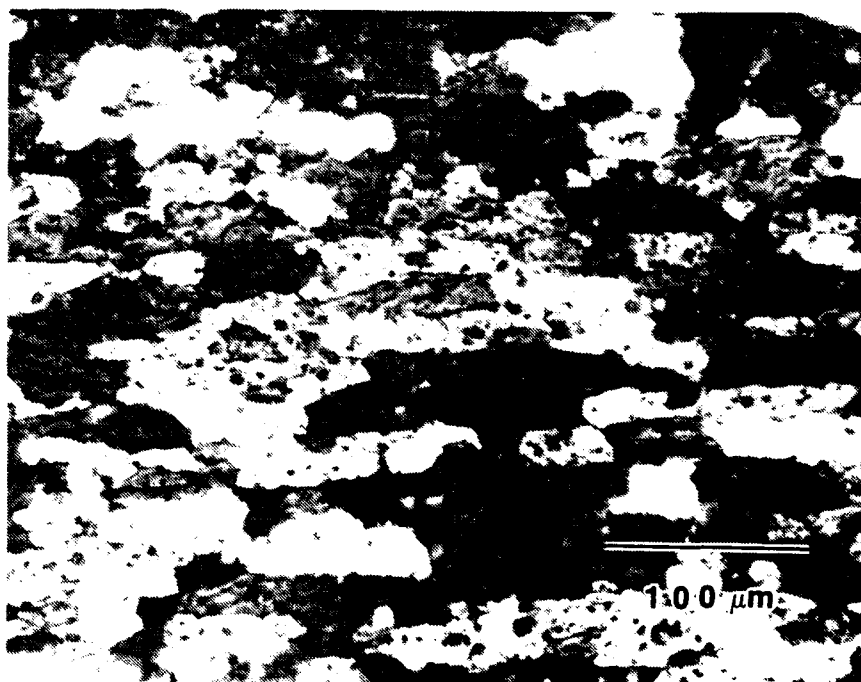
(a)
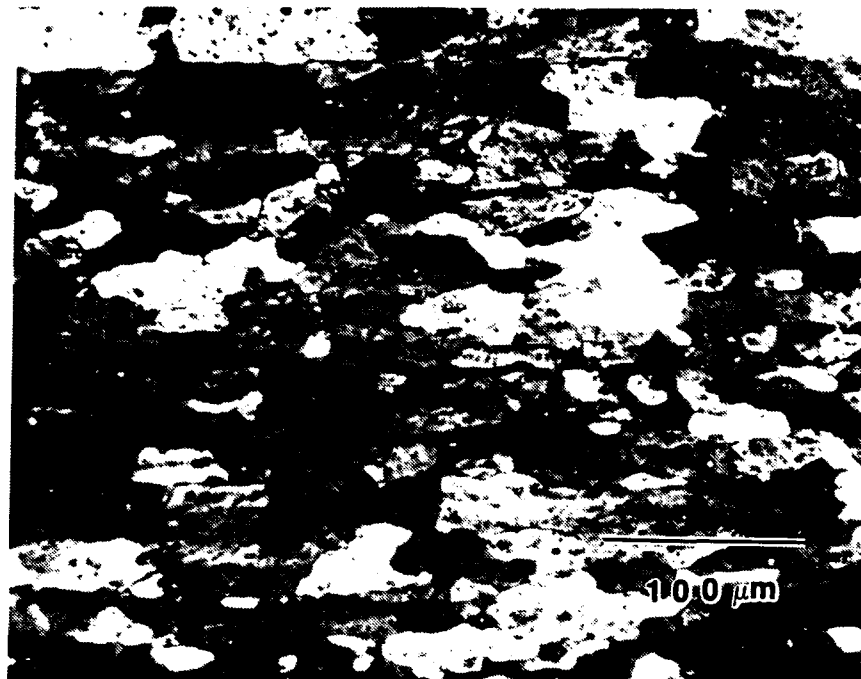
(b)

Figure 4.5 Optical Micrographs (x261), Showing grip sections of Al-Cu 2519 Alloy, Tensile Tested at $\dot{\epsilon} = 6.7 \times 10^{-4} s^{-1}$. (a) TMP A, Rolled at 300°C; (b) TMP B, Rolled at 350°C; (continued);
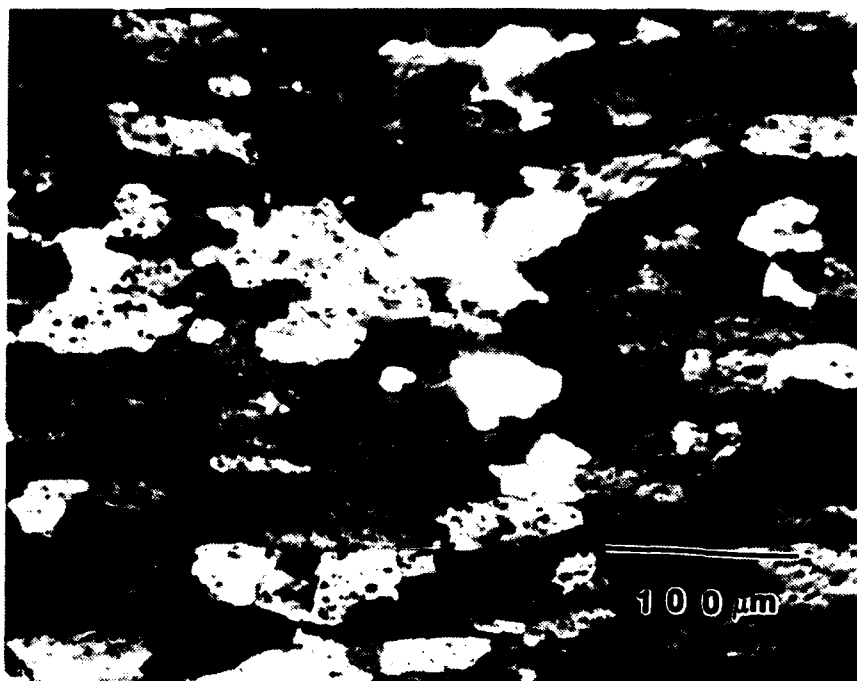
(c)

100 μm

Figure 4.5 (c) TMP C, Rolled at 400°C.

Figure 4.8 (a) is an SEM micrograph showing the Θ-phase particle size and distribution of a specimen overaged 50 hours. There appears to be a higher percentage of particles in the size range of 1-2 μm as compared to specimens aged for 10 hours, (see Figure 4.1 (a)). Figure 4.8 (b) is a typical optical micrograph of the overaged condition showing that coarse-grained microstructure is not discernibly different from that of the shorter overaging time (Figure 4.1 (b)). Figure 4.8 (c) is a typical micrograph showing the microstructure after rolling (TMP D) and annealing for five minutes at 450°C. The recrystallized grain size measuring 8.9 microns is appreciably smaller than the 11.1 μm grain size for TMP A shown in Figure 4.2 (c). This is consistent with the enhanced ductility and reduced strength observed in the mechanical property data.

3.   Reheating Time Effects

In an attempt to further refine the as-processed microstructure, TMP D was modified by reducing the reheating time between the first six rolling passes from 30 to 5 minutes. By reducing the reheating time, the material will have less time to recover between rolling passes. Subsequent rolling passes would then involve increased dislocation density and result in more stored strain energy within the material. Thirty-minute reheating intervals were used for rolling passes seven through nine to allow sufficient time for recovery as well as nucleation of recrystallization. Tensile test data comparing the response of the this material processed by TMP D or TMP E are provided in Figures 4.9 and 4.10. Results of the tensile testing indicates essentially no difference between material processed by TMPs D and E.
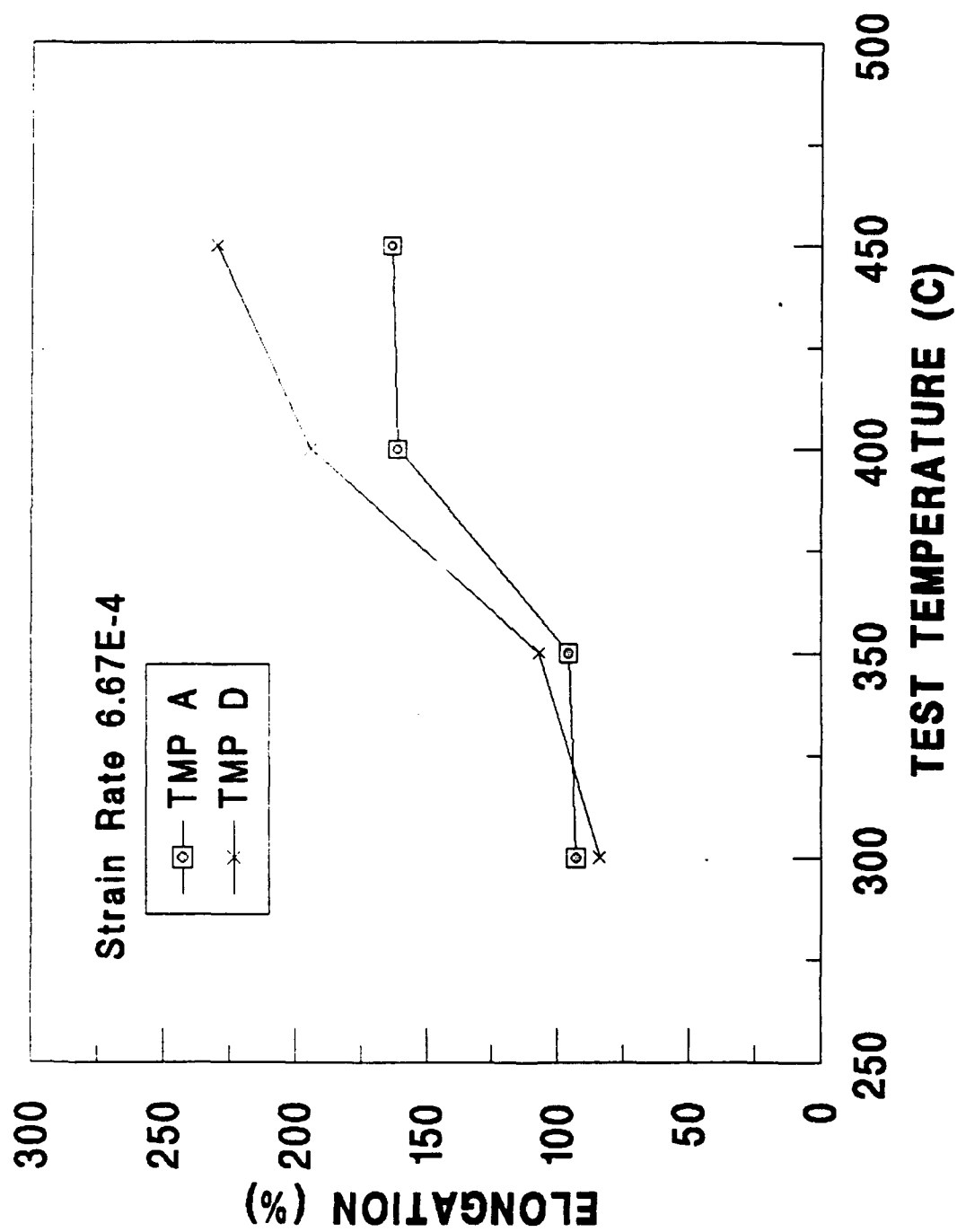
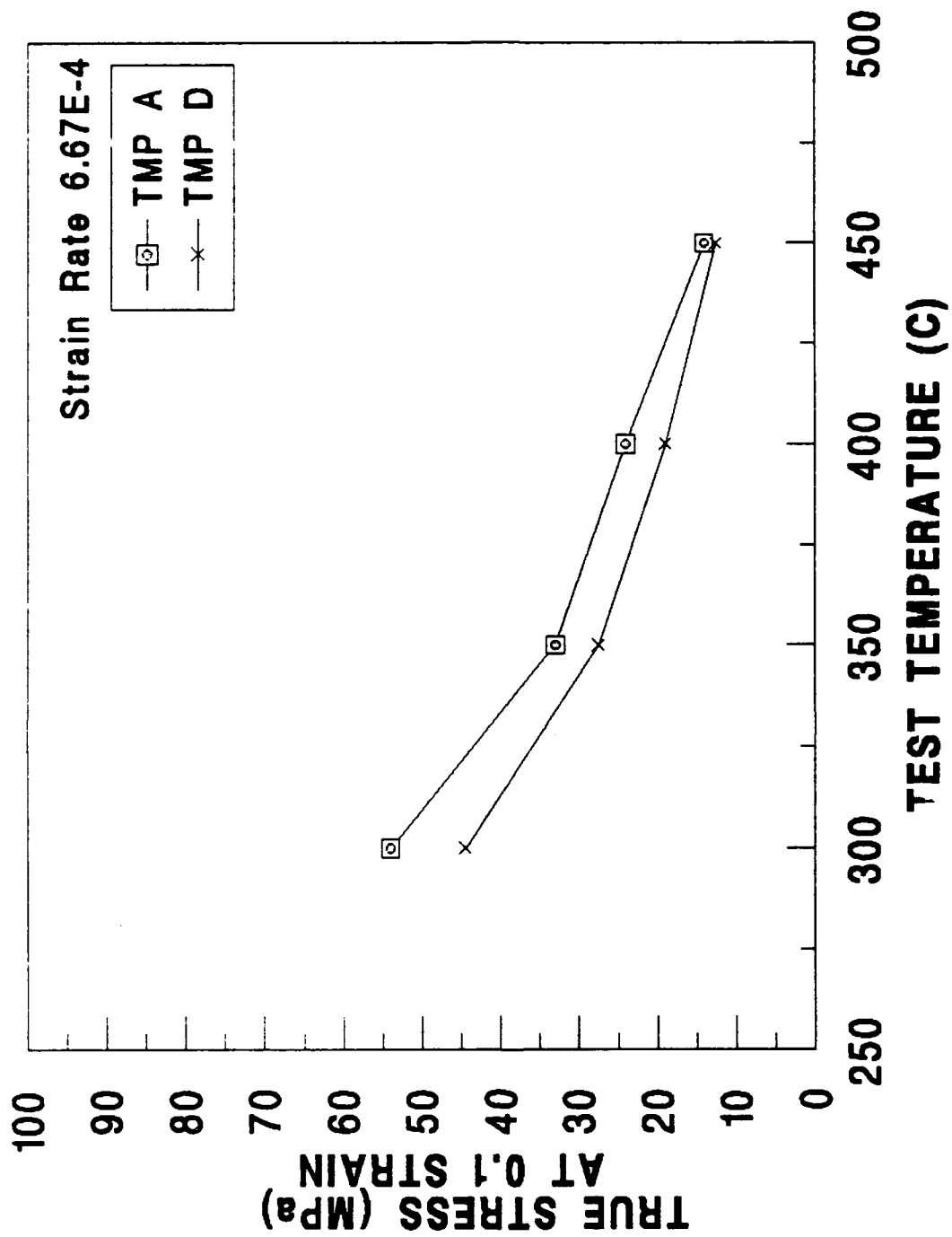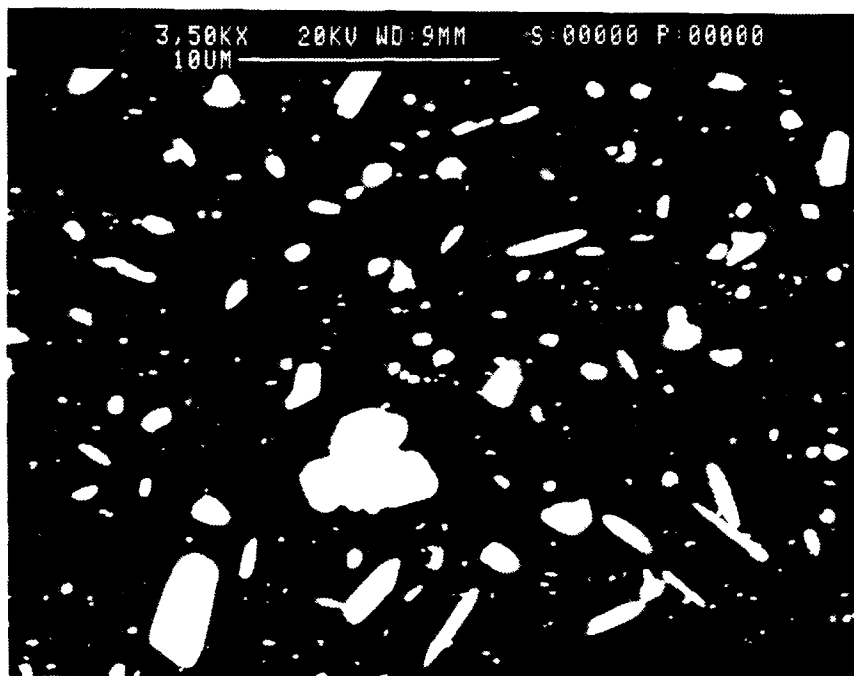Figure 4.6 Ductility vs. Test Temperature, TMP A and D.

40

Figure 4.7 True Stress at 0.1 Strain vs. Test Temperature, TMPs A and D.

(a)

(b)

Figure 4.8   Al-Cu 2519 Alloy, After Overaging for 50 Hours at 450°C. (a) SEM Backscattered Micrograph; (b) Optical Micrograph (x105); (continued);
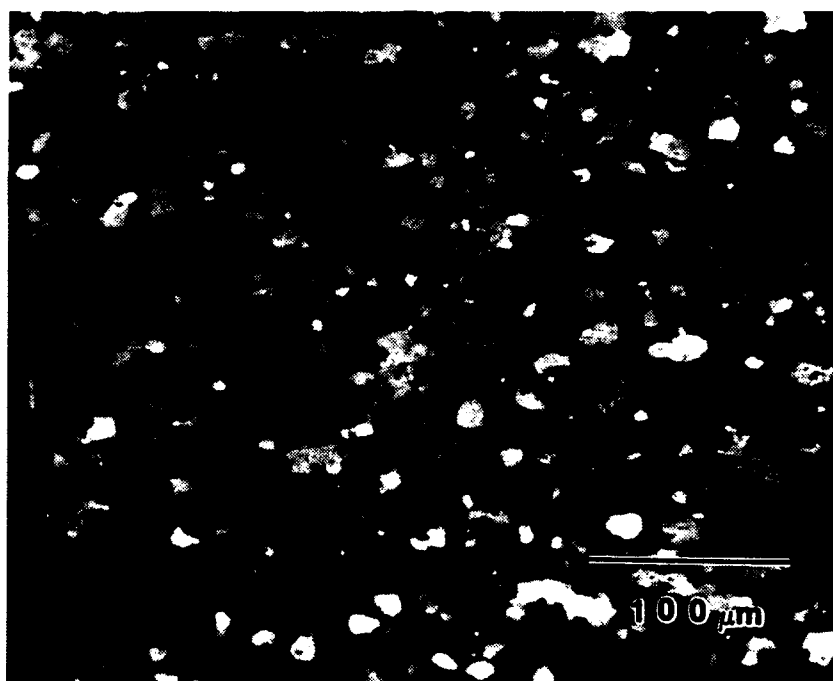
(c)

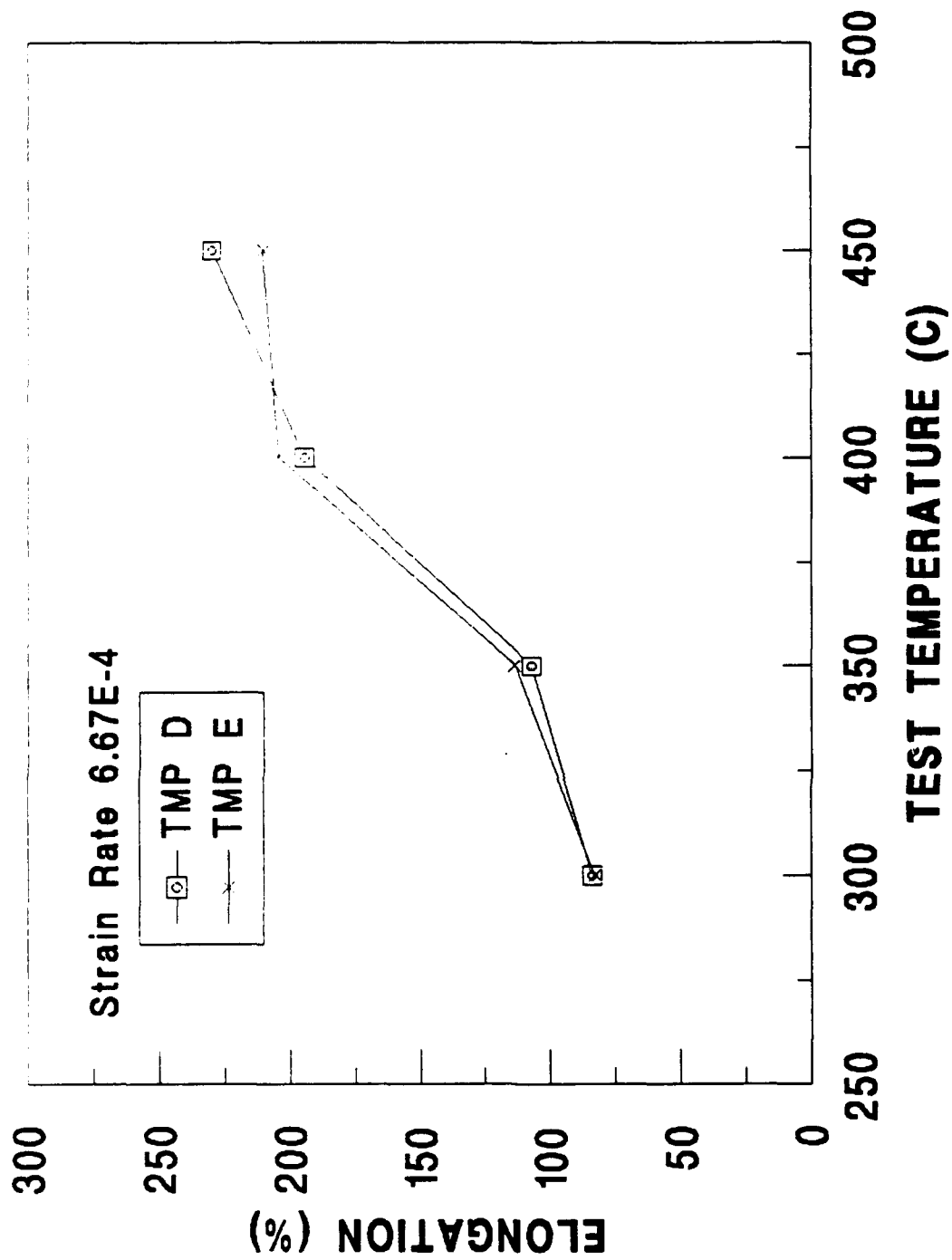Figure 4.8 (c) Optical Micrograph (x261), 5 min., 450°C Post TMP D Anneal.

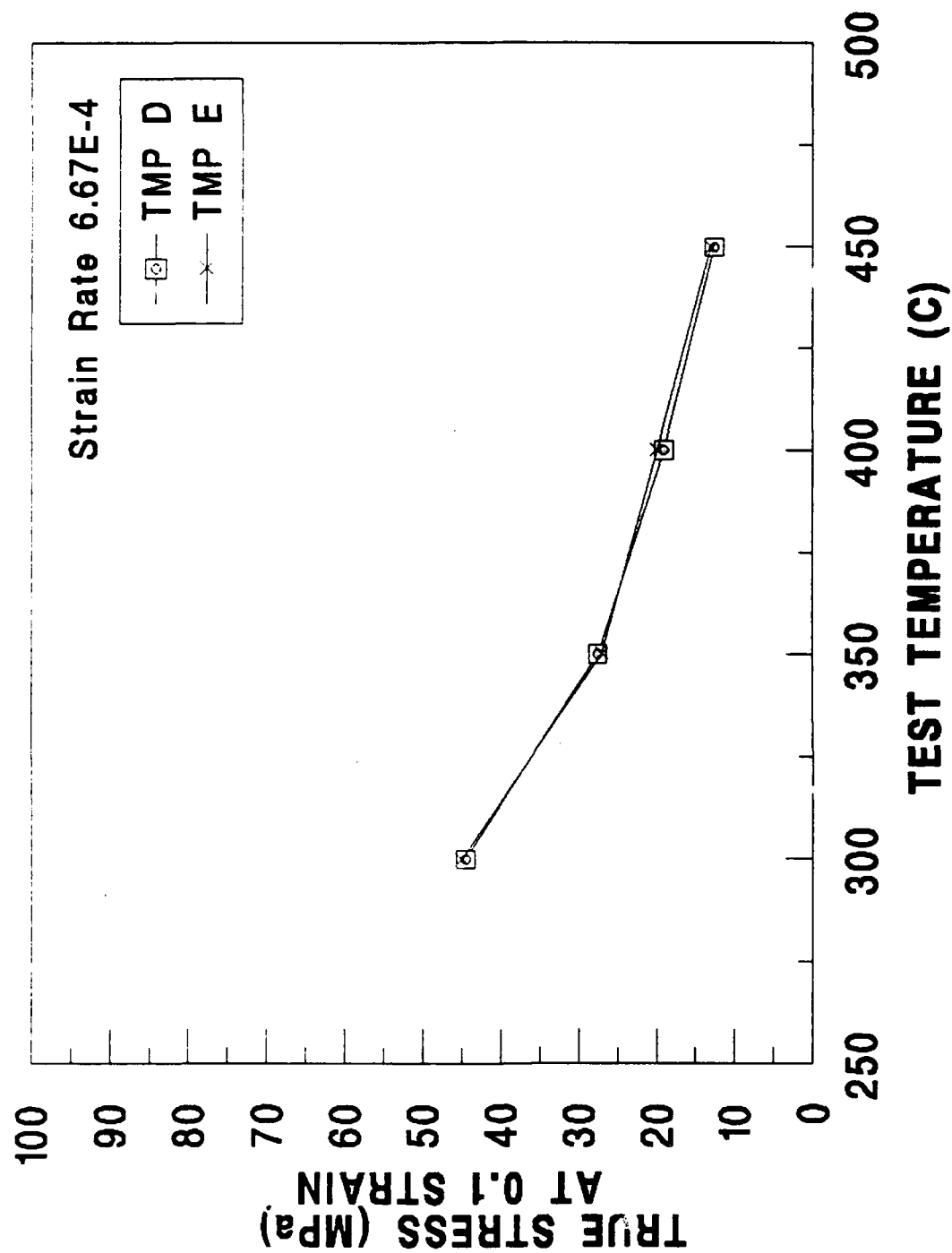Figure 4.9 Ductility vs. Test Temperature, TMPs D and E.

44

Figure 4.10 True Stress at 0.1 Strain vs. Test Temperature, TMPs D and E.

Figure 4.11 is a typical optical micrograph of the microstructure upon annealing at 450°C for five minutes after completion of TMP E. The microstructure is not discernible different from that obtained from TMP D (shown in Figure 4.8 (c)). Data obtained for TMP D and TMP E grain sizes provided values of 8.9 and 8.5 μm, respectively. This small apparent difference in grain size is consistent with the minimal differences in mechanical property data.

From this, it is concluded that reducing the reheating times between the first six rolling passes of the thermomechanical process has not produced an appreciable difference in the microstructure, grain size, or mechanical properties of this material.

4. Effects of Annealing after Rolling

a. Annealing Temperature

A representative microstructure after rolling at 300°C was shown in Figure 4.2 (b). Comparisons among microstructures immediately after rolling were not enlightening. Rolled samples were subsequently annealed at each of the tensile test temperatures in an attempt to reveal microstructural differences that could be used to assess the effects of the TMP. Polarized light microscopy for samples annealed at 300 and 350°C also were not informative and an apparently unrecrystallized microstructure remained. However, micrographs of samples annealed at 400 and 450°C provided polarized light micrographs which revealed clear grain structures.

Additionally, optical micrographs (without polarized light) for samples processed by TMP B and annealed for 35 minutes at either 300 or 450°C, are shown in
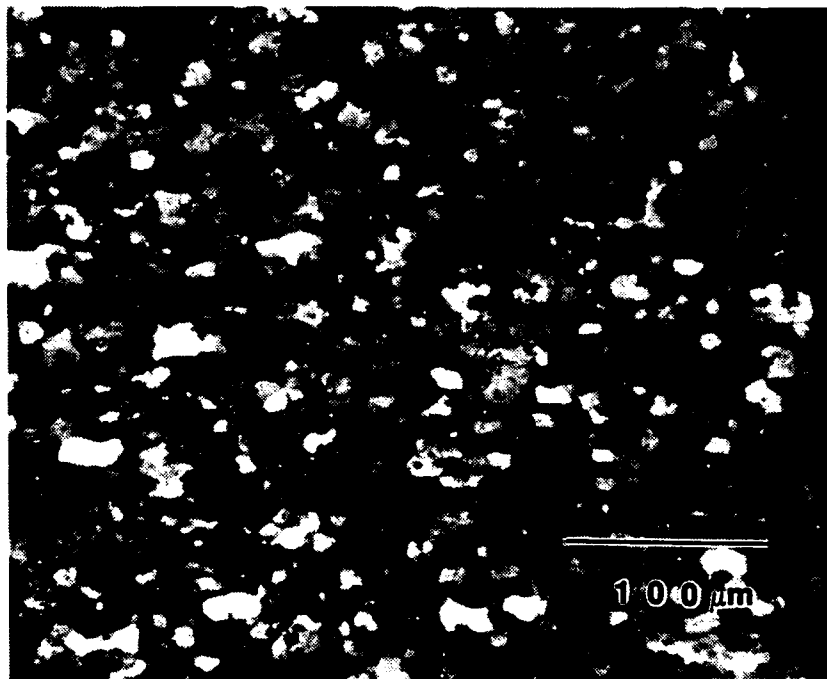
Figure 4.11 Optical Micrograph (x261), 5 min., 450°C Post TMP E Anneal.

Figures. 4.12 (a) and (b) respectively. At the higher annealing temperature, the micrograph appears clearer, with fewer fine precipitate particles. The reduced number of fine precipitate particles in the sample annealed at 450°C likely assists the clarity of subsequent polarized light micrographs.

b.   Annealing Time

Samples processed by TMP E were annealed at 450°C for either 5, 35 or 120 minutes. Grain size measurements from optical micrographs indicated grain sizes of 8.4, 10.2 and 12.4 μm, respectively. Thus, the grains grow and could also be expected to coarsen during tensile testing at elevated temperatures.

c.   Tensile Tests

To assess the effects of annealing at higher temperatures to achieve recrystallized grain structures prior to tensile testing at lower temperatures, samples processed by TMP E were annealed at 400°C for seven minutes and subsequently tensile tested at 300 and 350°C. This procedure was designated TMP F. Samples annealed at 450°C for seven minutes were tensile tested at 300, 350 and 400°C, and this procedure was designated TMP G. Tensile testing results for TMP's E, F, and G are shown in Figures 4.13 and 4.14.
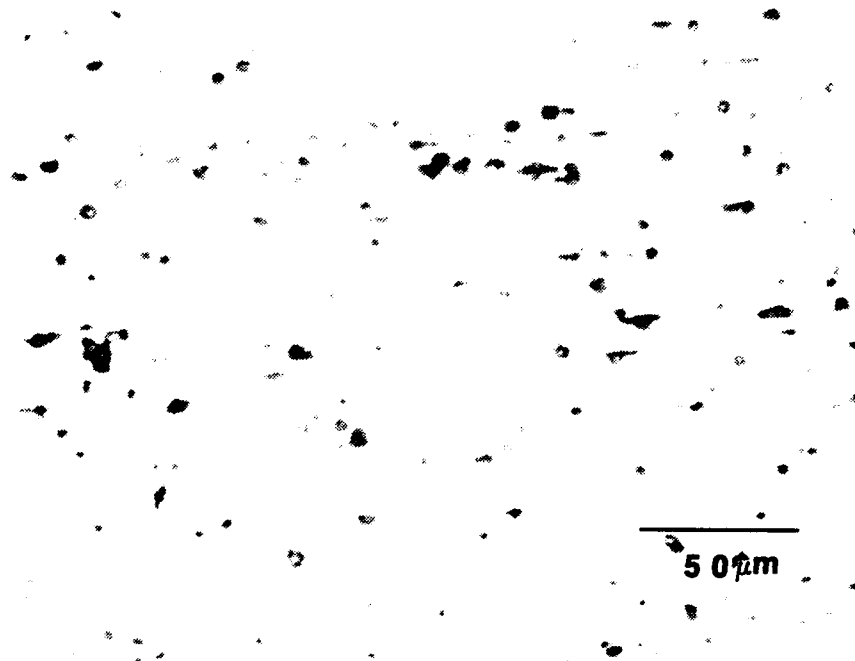
(a)
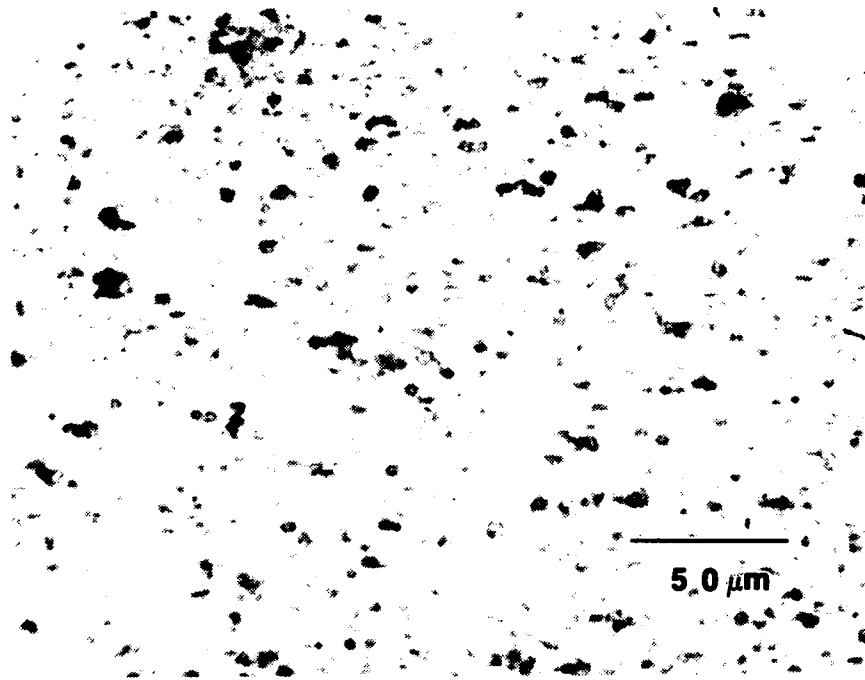
(b)

Figure 4.12 Optical Micrograph (x420), 35 min., TMP B. (a) Annealed at 300°C; (b) Annealed at 450°C.
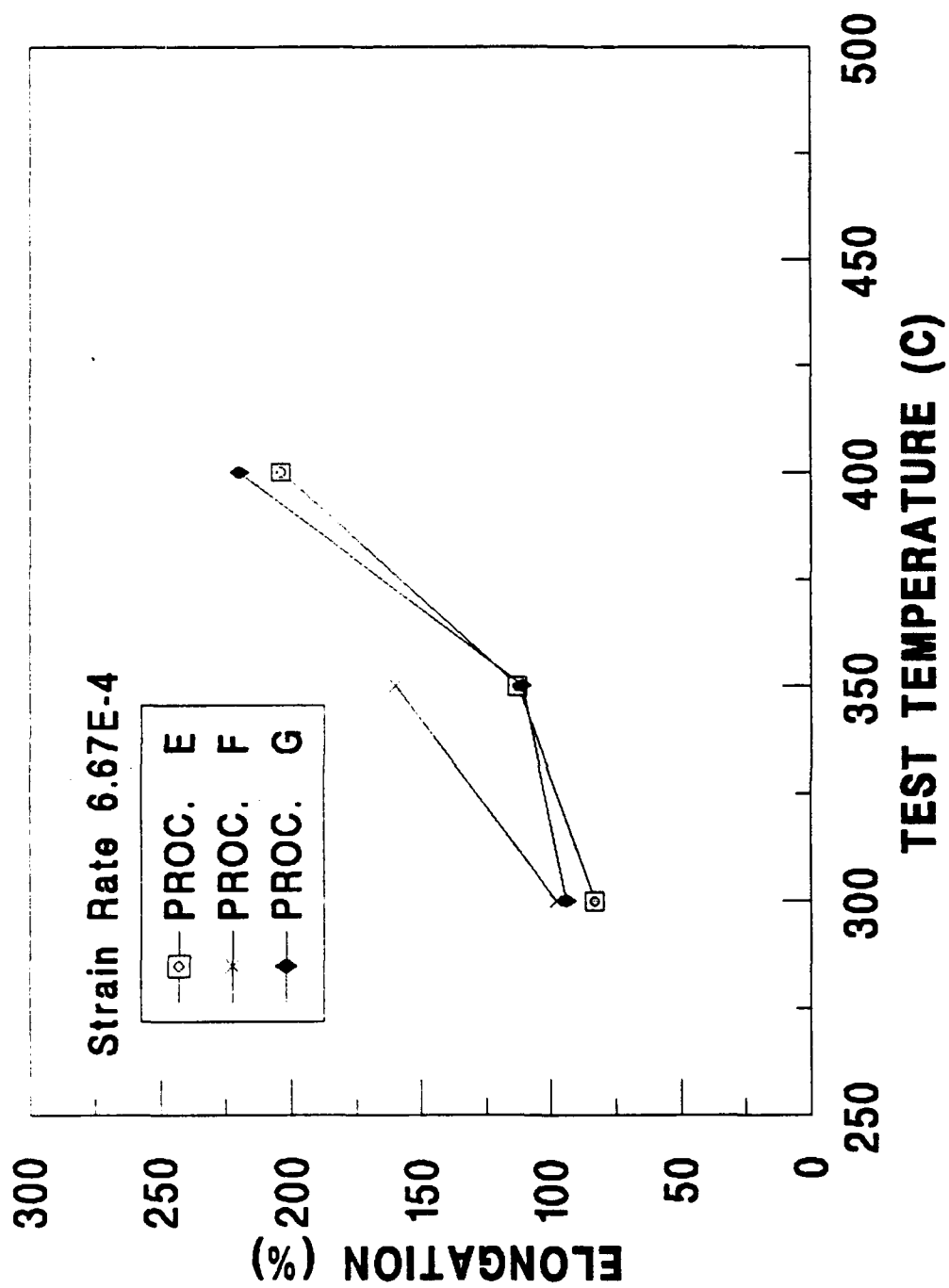
49

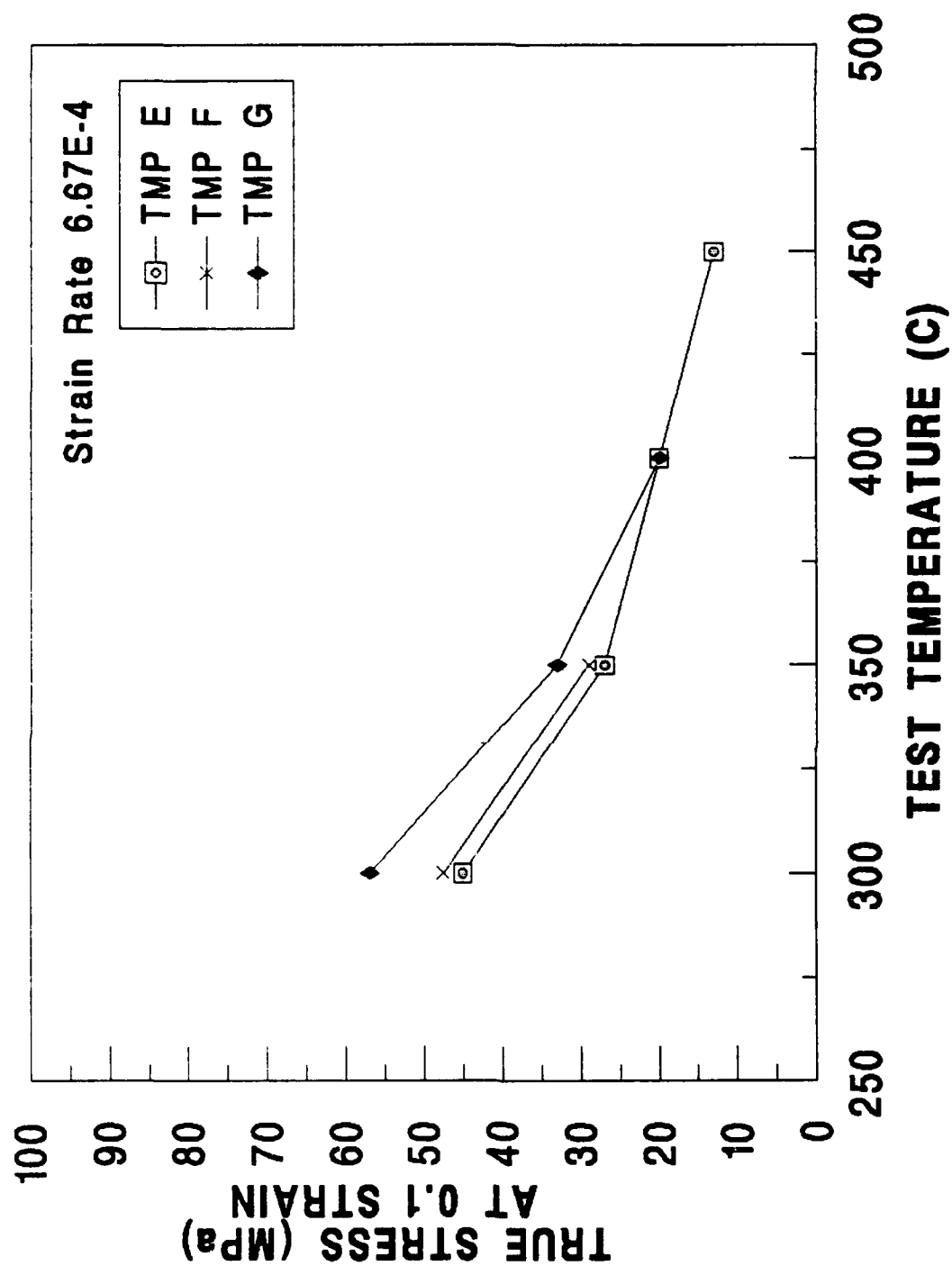Figure 4.13 Ductility vs. Test Temperature, TMPs E, F and G.

Figure 4.14   True Stress at 0.1 Strain vs. Test Temperature, TMPs E, F and G.

51

D. DISCUSSION

This work on Al-Cu alloy 2519 has attempted to develop a fine, equiaxed microstructure similar to the microstructures developed in the superplastic Al-Mg alloys also studied at NPS. Here the processing resulted in microstructures consisting of distributions of Θ phase particles with the largest particles of size 1-3 μm. Precipitate particles of this size have been shown to serve as sites for nucleation of recrystallization [Ref. 18].

The theory of PSN was developed to describe the role of second-phase particles during recrystallization. It is well-established that a distribution of very fine precipitate particles (e.g., 10-100 nm in size) serves to retard dislocation motion. Processing with such a fine dispersion would result in an increase in dislocation density but also in inhibition of recrystallization due to retardation of recovery and substructure formation. As particle size increases, the nature of effect of the particles on the deformation state in the material changes. This is thought to occur at a critical particle size $d_{critical} \approx$ 1-2 μm [Ref. 18] depending upon the strain, the temperature of deformation and the physical characteristics of the particles. Particles larger than $d_{critical}$ develop deformation zones when subjected to large strains. In these zones, high dislocation densities result in fine cell or subgrain structures providing local lattice rotations. These deformation zones, in turn, become favorable sites for nucleation of recrystallization. Figure 4.15 shows the relationship between $d_{critical}$ and strain. Here, the strain would be that achieved on a given rolling pass in the schedule used. The value of $d_{critical}$ decreases as the magnitude of the

strain per pass increases. An understanding of this relationship is a key consideration is the development of TMP for a refined microstructure able to support superplasticity.
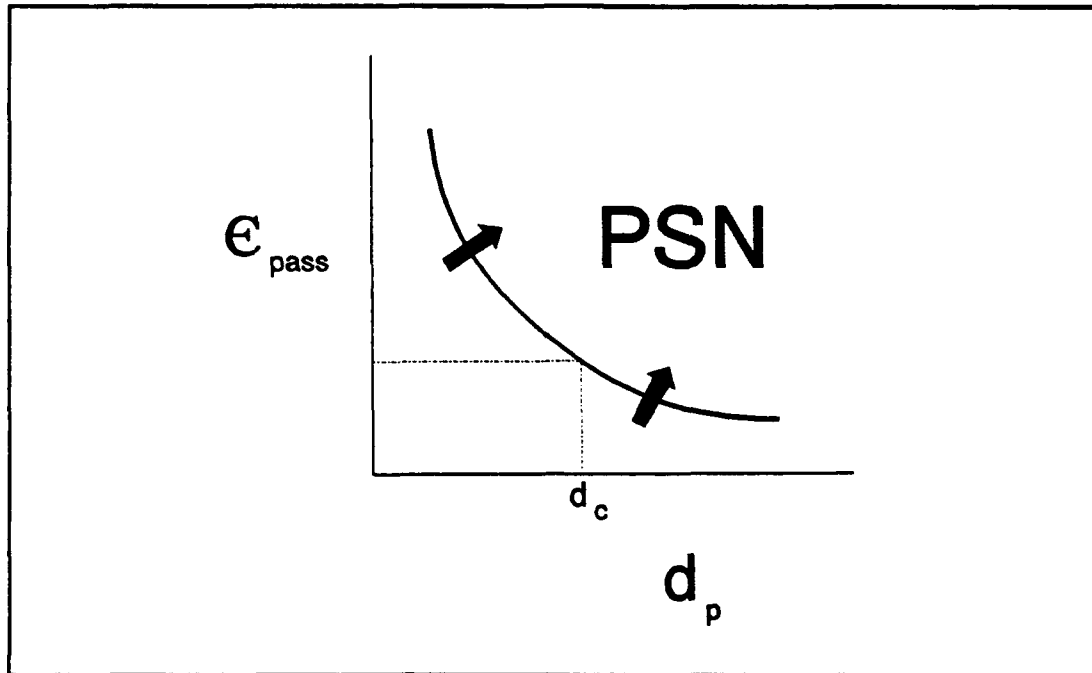

Figure 4.15 PSN as a Function of Strain per Rolling Pass and Precipitate Size.

For this Al-Cu alloy, a random distribution of 1-2 μm Θ-phase particles were produced by a pre-strain and overaging treatment of 10 hours duration. The overaged material was theromomechanically processed using a schedule calling for increasing strain during the rolling schedule, with strain per pass reaching ≈ 0.5 on the final pass. These two conditions (particles > $d_{critical}$ and a large strain) are thought to provide the necessary conditions to produce a fine grained microstructure via PSN, either during TMP or during deformation at elevated temperatures.

Results, however, indicate that the material has not fully recrystallized during the TMP. A recrystallized microstructure with grain size ≈ 11.1 μm was obtained by

53

annealing at 450°C after TMP. Apparently, not all precipitate particles provided nucleation sites for recrystallization. A finer grain size would be anticipated had all particles done so. The particles are distributed in size about an average or mean particle diameter. Figure 4.16 is an illustration showing a distribution of particles about a mean and how the number of particles that exceed $d_{critical}$ is increased when the distribution is shifted toward a larger mean particle size. It is assumed that $d_{critical}$ is the same for both distributions, reflecting a constant rolling schedule as employed here. This shift in particle size distribution with respect to a $d_{critical}$ results in a larger number of particles participating in PSN. By increasing the overaging time from 10 to 50 hours, more precipitate particles formed and existing particles coarsened. Thus, the distribution of particles size was shifted to the right in a manner similar to that shown schematically in Figure 4.16. The recrystallized grain size upon annealing at 450°C was reduced to ≈ 8.9 μm and the mechanical test data indicated significant increase in ductility.

Further application of PSN theory would suggest that lower rolling temperatures would produce higher dislocation densities and result in a finer recrystallized microstructure. However, no apparent difference in grain size or mechanical properties were detected over the range of rolling temperatures used. By extending the range of rolling temperatures or taking multiple samples for each test condition small differences may become apparent.

Reducing the reheating interval between rolling passes for the first six passes was an additional attempt to increase the stored strain energy and dislocation density within the material. Results indicated only a slight decrease in grain size and no apparent change
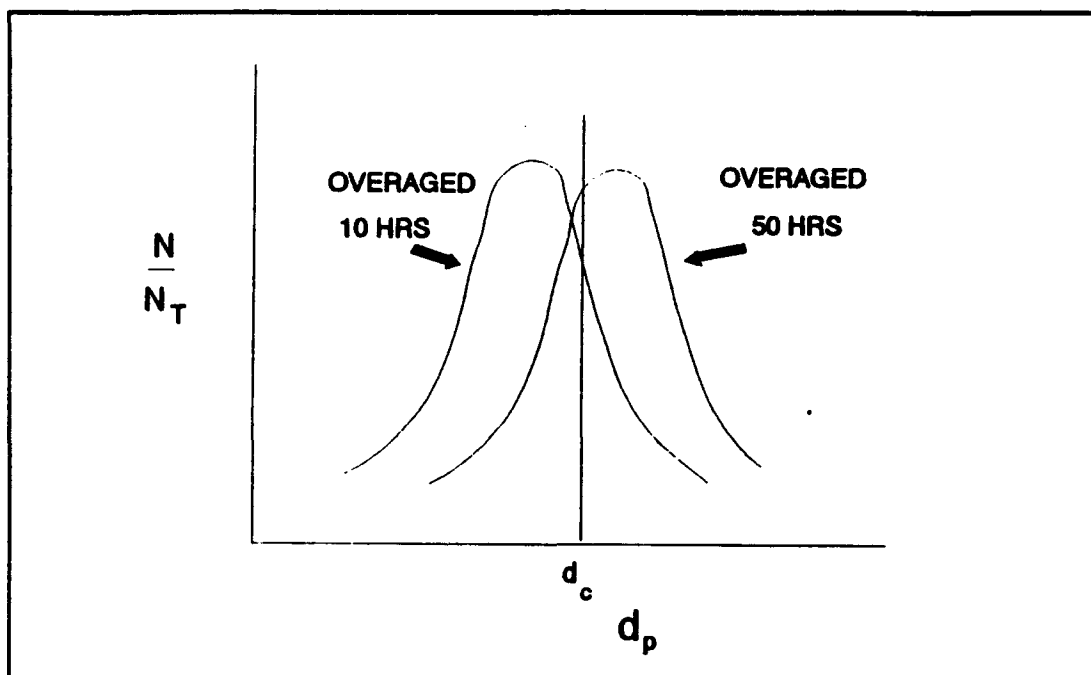
Figure 4.16 Precipitate Size Distribution.

in mechanical properties. The change in TMP again may not be sufficient to yield decisive change. Also, the changes made to the TMP or to the overaging treatment have either attempted to increase particle size or increase dislocation density, effectively reducing $d_{critical}$. Attempts to modify the TMP by just increasing particle size or increasing dislocation density may not produce the desired result of a more refined microstructure. More severe strains may also lead to shearing of precipitate particles effectively reducing particle size and nullifying and beneficial benefit from increasing dislocation density.

The microscopy shows clear evidence that the TMP refines the grain size. The observation of reduced grain size with increase particle size suggests that PSN is the mechanism by which grains are refined. However, PSN theory assumes site saturation of nucleation and growth until impingement with other grains. This resulting

microstructure is considered to be the final step and does not consider grain growth. Grain growth does in fact occur and likely has also contributed to the limited ductility achieved thus far. Attempts to produce a recrystallized microstructure prior to tensile testing did not produces significant results and continued analysis may indicate grain growth had occurred. Additional modifications to the TMP are necessary to produce not only a fine but also a stable grain size in Al-Cu 2519. Also the theory of PSN needs to be developed further with consideration toward incorporating grain growth.

V. CONCLUSIONS

A variety of thermomechanical processing techniques have been employed to determine the superplastic response of aluminum alloy 2519 at elevated temperatures. Conclusions drawn from the present study are as follows:

1. Thermomechanical processing followed by annealing at 450°C produced a refined microstructure with grains of size ≈ 8-10 μm.

2. A 10 pct. pre-strain followed by overaging for 10 hours at 450°C resulted in a uniform distribution of Θ phase particles with the largest particles achieving a size ≈ 1-2 μm.

3. Increasing the overaging time from 10 hours to 50 hours, resulted in a uniform distribution of particles, with a significantly larger number of particles achieving a size > 1 μm.

4. By increasing the number of Θ-phase particles of sufficient size capable of PSN, a more refined microstructure was obtained and ductility was enhanced.

5. The rolling temperature of the TMP had no apparent effect on the recrystallized grain size or mechanical properties.

6. Static annealing at 450°C indicated that grains recrystallized to a size ≈ 8 μm, but subsequently grew to over 12 μm over a two hour period. This suggests that recrystallized grains, perhaps fine enough to produce a superplastic response, are unstable, resulting in grain growth and a limited superplastic response of the material.

7. Recrystallized grains of grip sections of deformed specimens revealed grains of size ≈ 18-19 μm. Indicating that grains grow over time during elevated temperature testing.

8. The limited superplastic response (260 pct.) achieved was the result of an unstable microstructure experiencing grain growth during elevated temperature testing.

9. There were no significant differences between samples rolled with 30 minute reheating interval between all rolling passes and those with 5 minute reheats between the first six passes and 30 minute reheats between passes seven through nine.

10. Samples aged for 50 hours, rolled at 300°C and reheated for 5 minutes between the first six passes and 30 minutes between passes seven through nine and subsequently annealed for 7 min. at 400°C prior to testing at 300°C and 350°C resulted in small improvements in ductility.

VI. RECOMMENDATIONS

The following recommendations are made for further study:

1. Increase the overaging time to 100 hours to determine if further changes in particle size distribution is observed.

2. Reduce the rolling temperature to 200°C to assess the effects of lower process temperatures during TMP.

3. Extend test temperatures to 500°C to determine the optimum temperature for future tensile testing.

4. Determine microstructural evolution of specimens placed in pre-heated grips and subsequently heated to test temperature.

5. Quantify particle size and grain size measurements by statistical analysis.
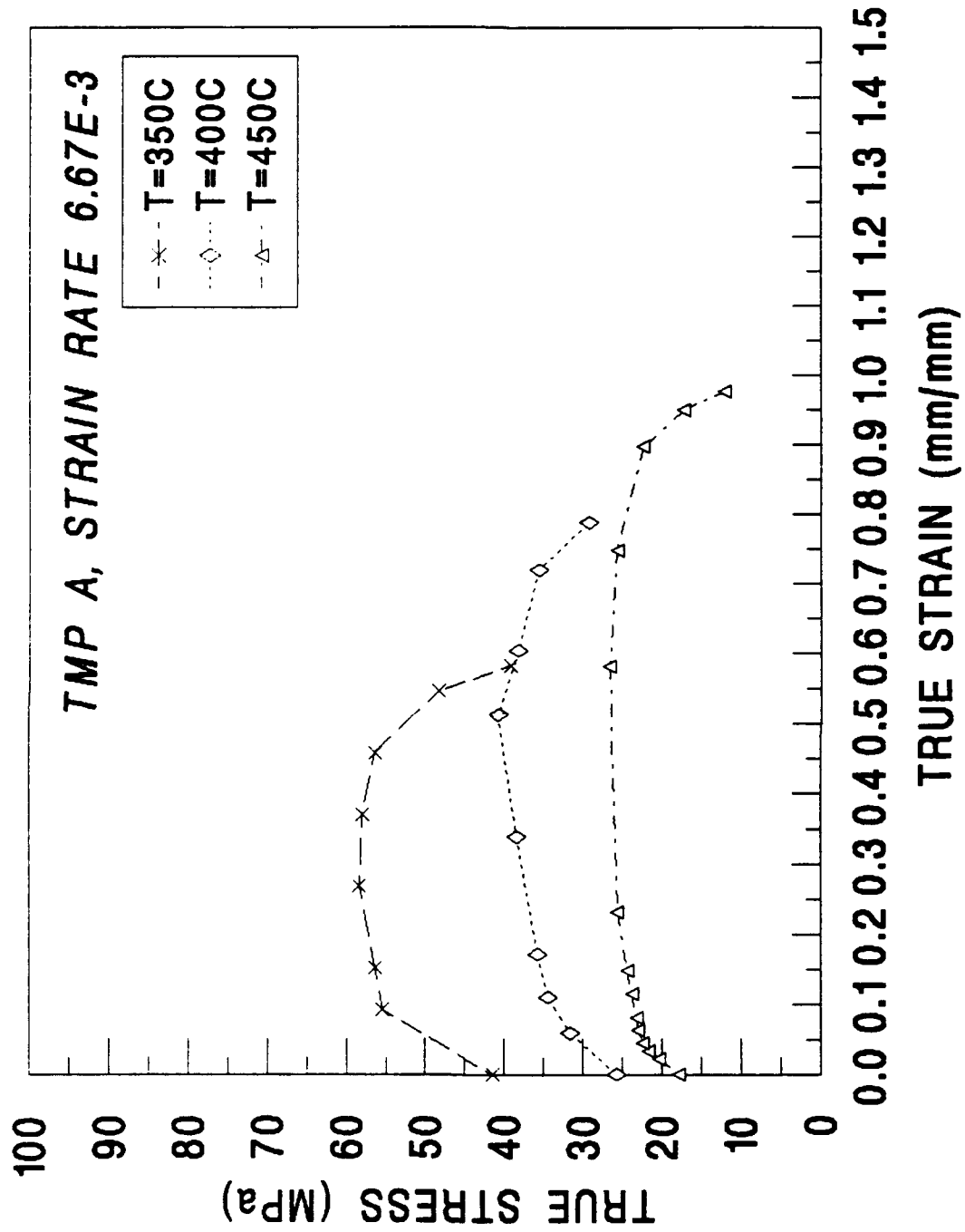
APPENDIX A: TRUE STRESS VS. TRUE STRAIN GRAPHS

Figure A.1 TMP A, $\dot\varepsilon = 6.67 \times 10^{-3}$ s^{-1}.

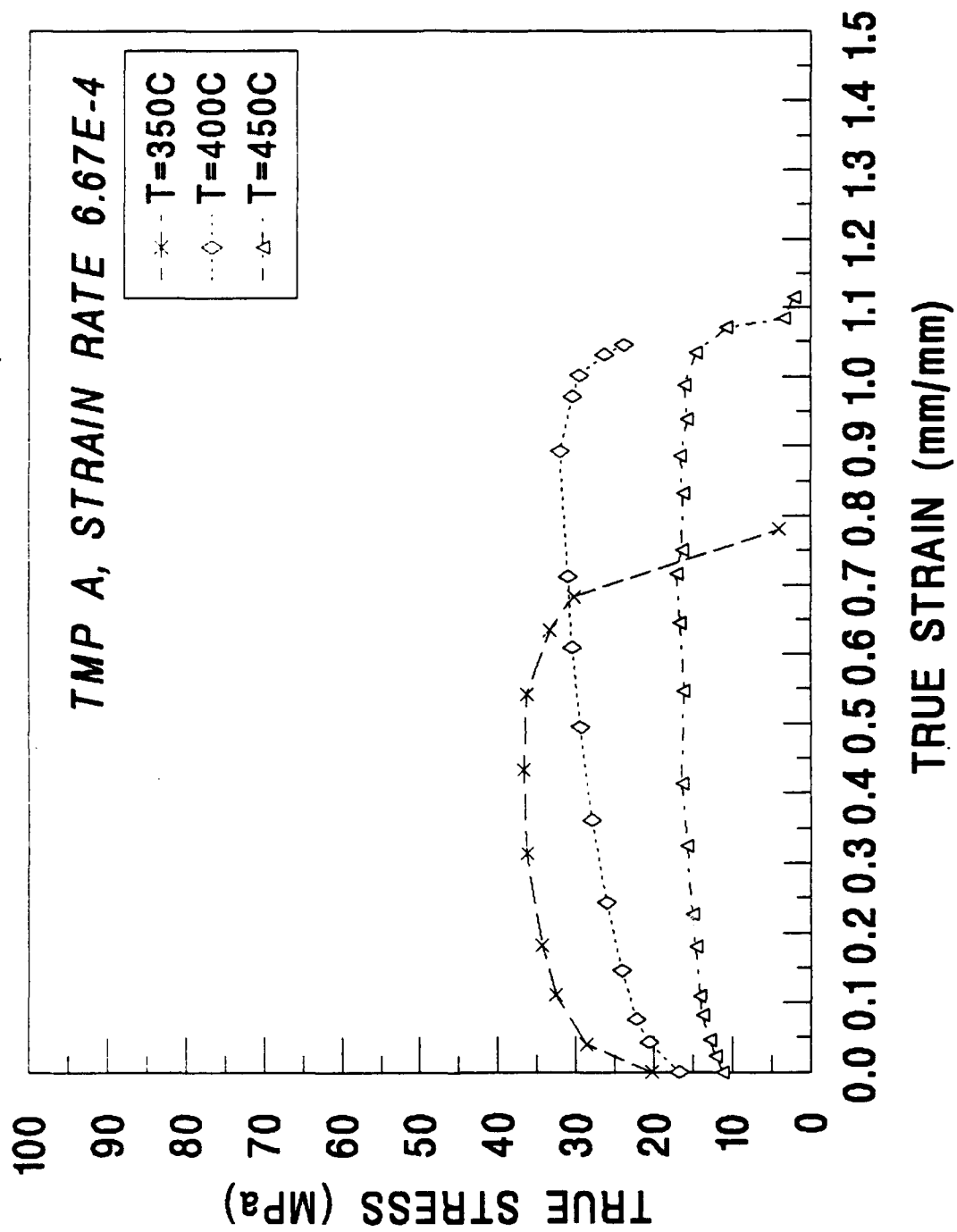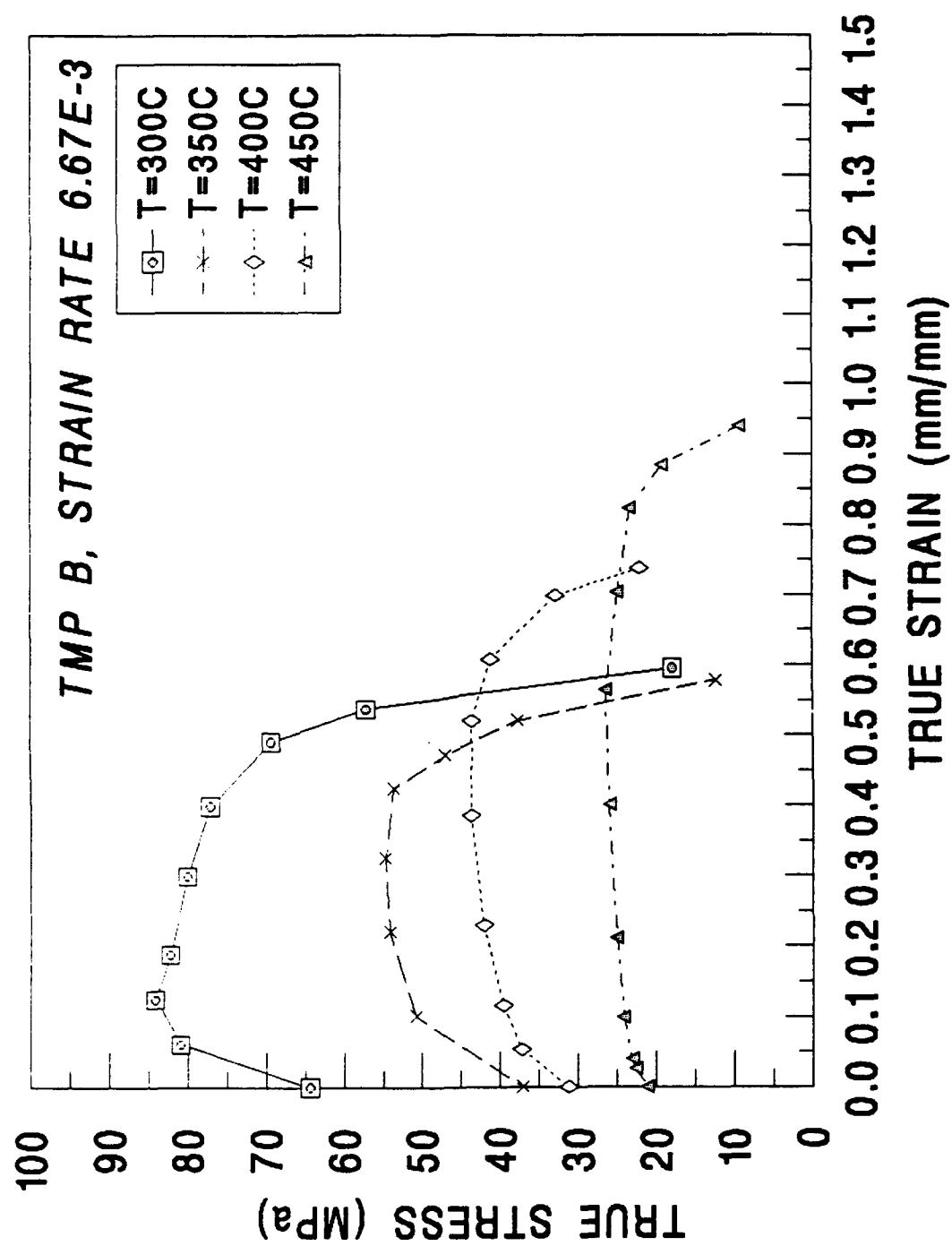Figure A.2 TMP A, $\dot\varepsilon = 6.67 \times 10^{-4}$ s^{-1}.

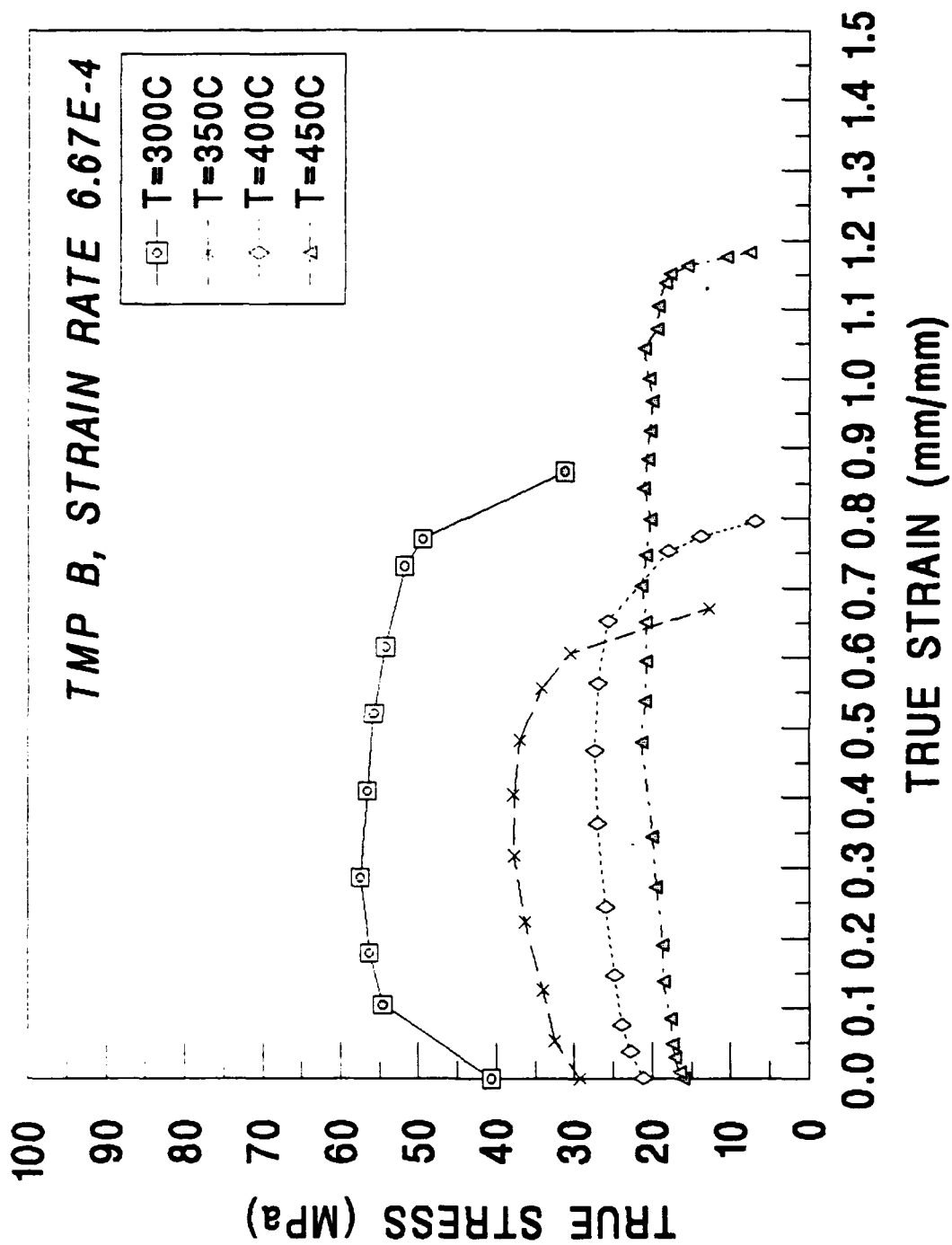Figure A.3 TMP B, $\dot{\epsilon} = 6.67 \times 10^{-3}$ s^{-1}.

Figure A.4 TMP B, $\dot{\epsilon} = 6.67 \times 10^{-4}$ s^{-1}.

Figure A.5 TMP C, $\dot{\epsilon} = 6.67 \times 10^{-3}$ s^{-1}.
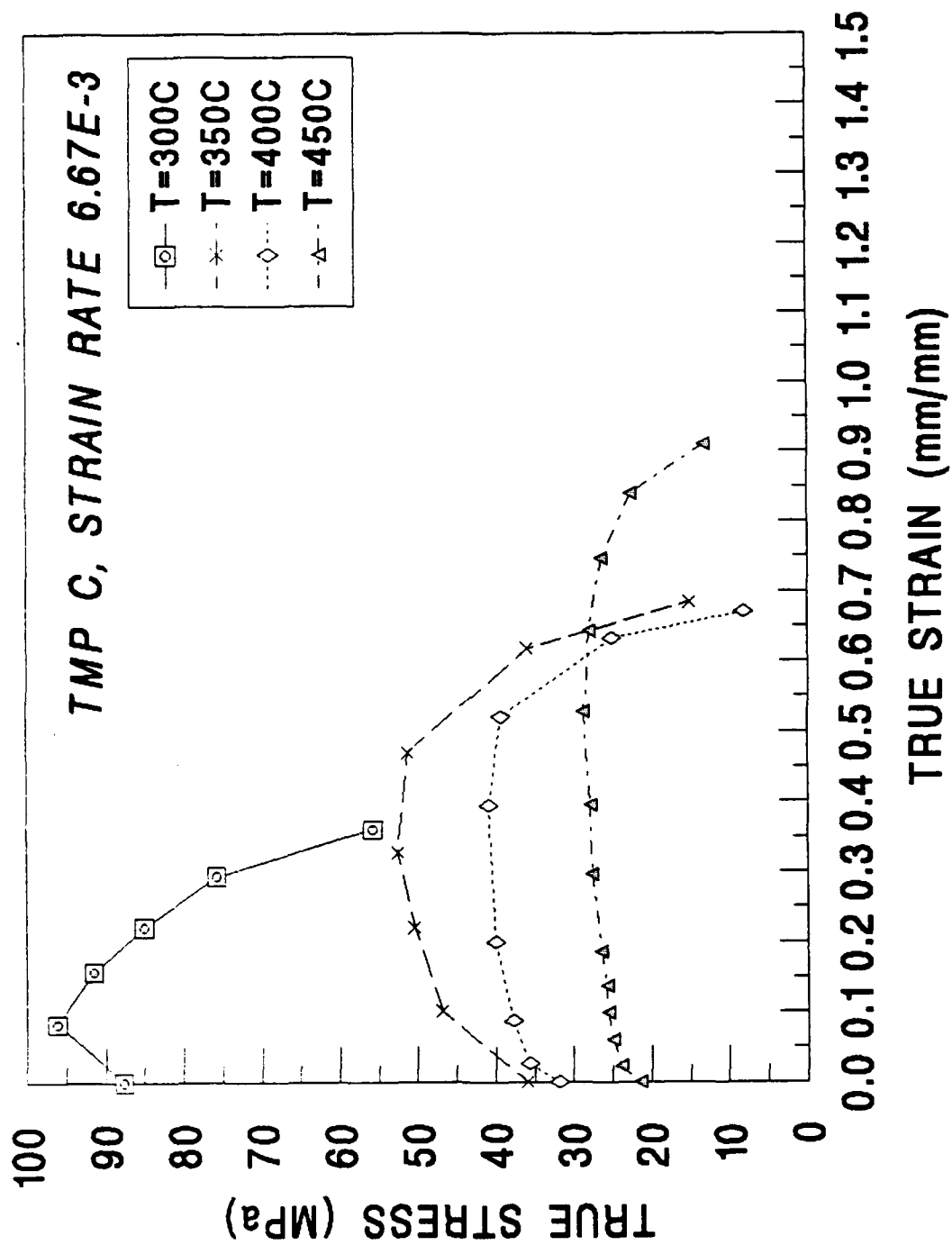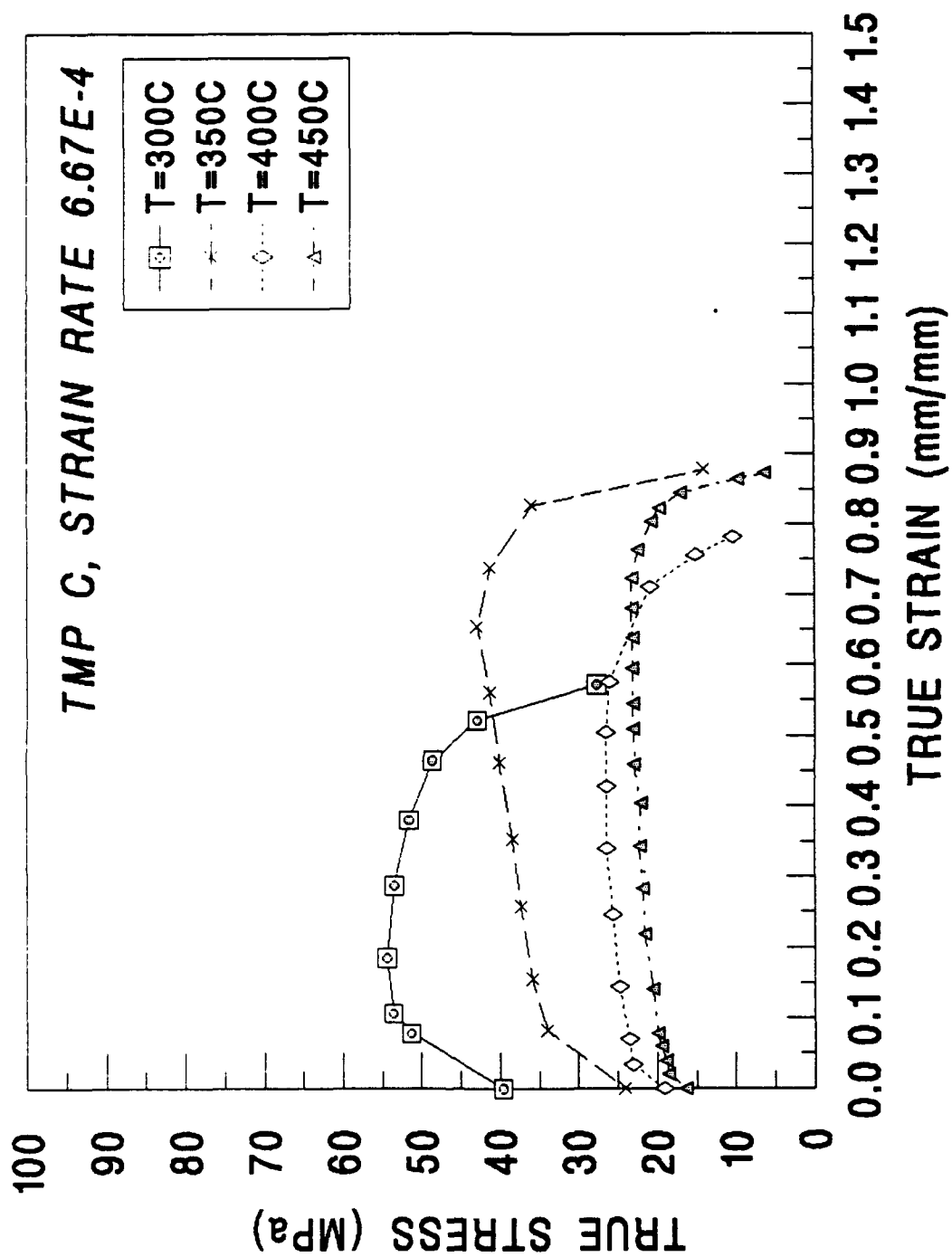
Figure A.6 TMP C, $\dot{\epsilon} = 6.67 \times 10^{-4}$ s^{-1}.
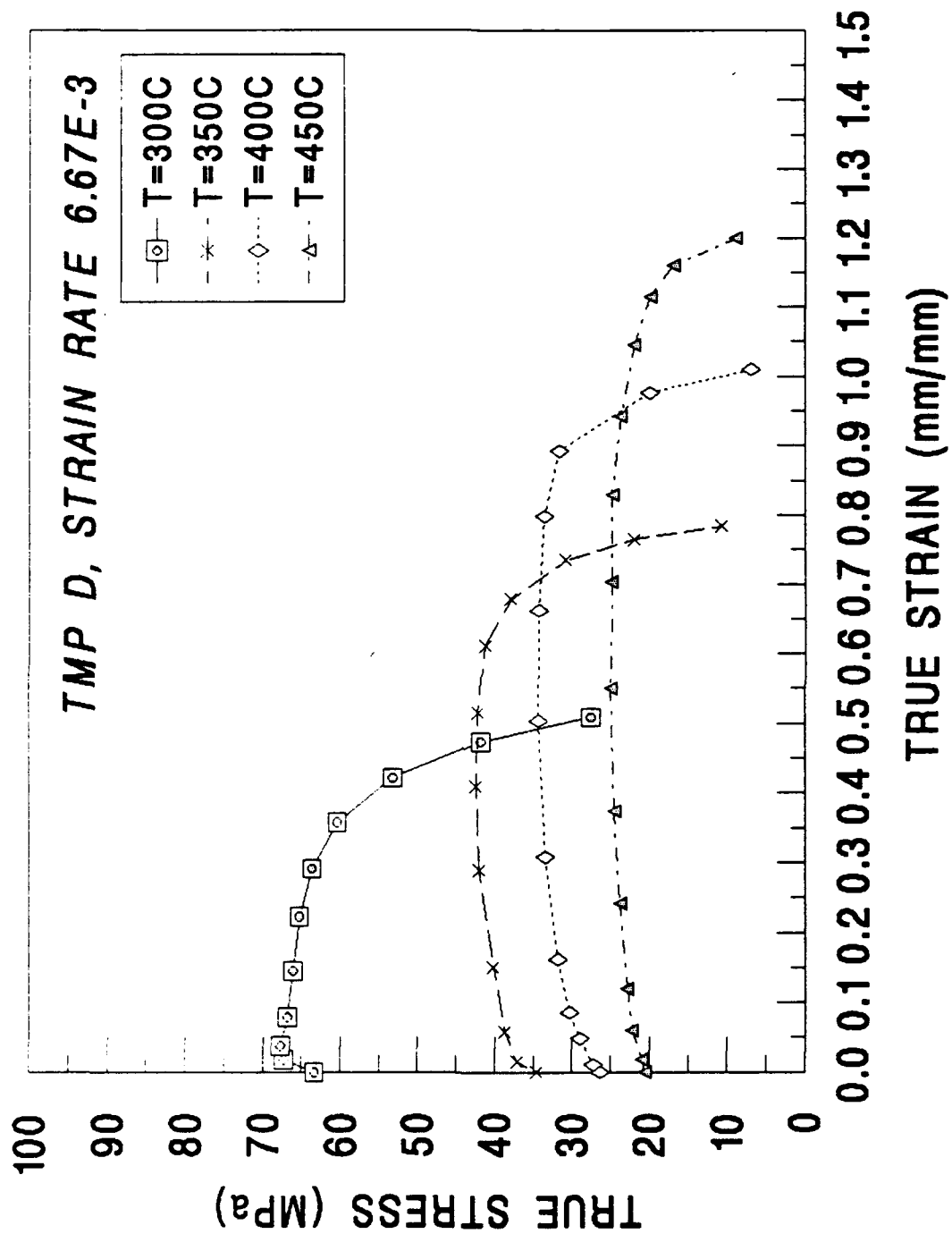
Figure A.7 TMP D, $\dot{\epsilon} = 6.67 \times 10^{-3}$ s^{-1}.

67

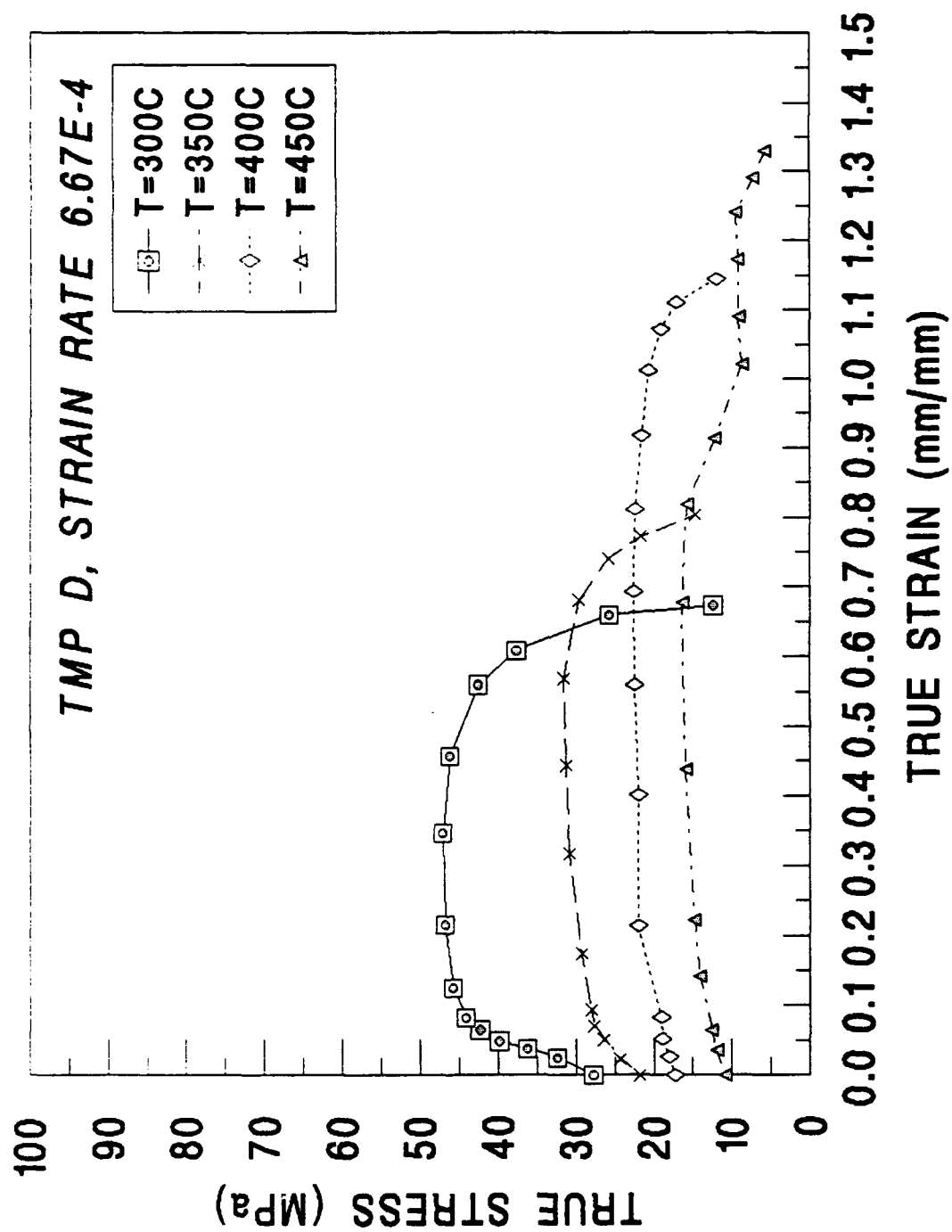Figure A.8   TMP D, $\dot{\varepsilon} = 6.67 \times 10^{-4}$ s^{-1}.
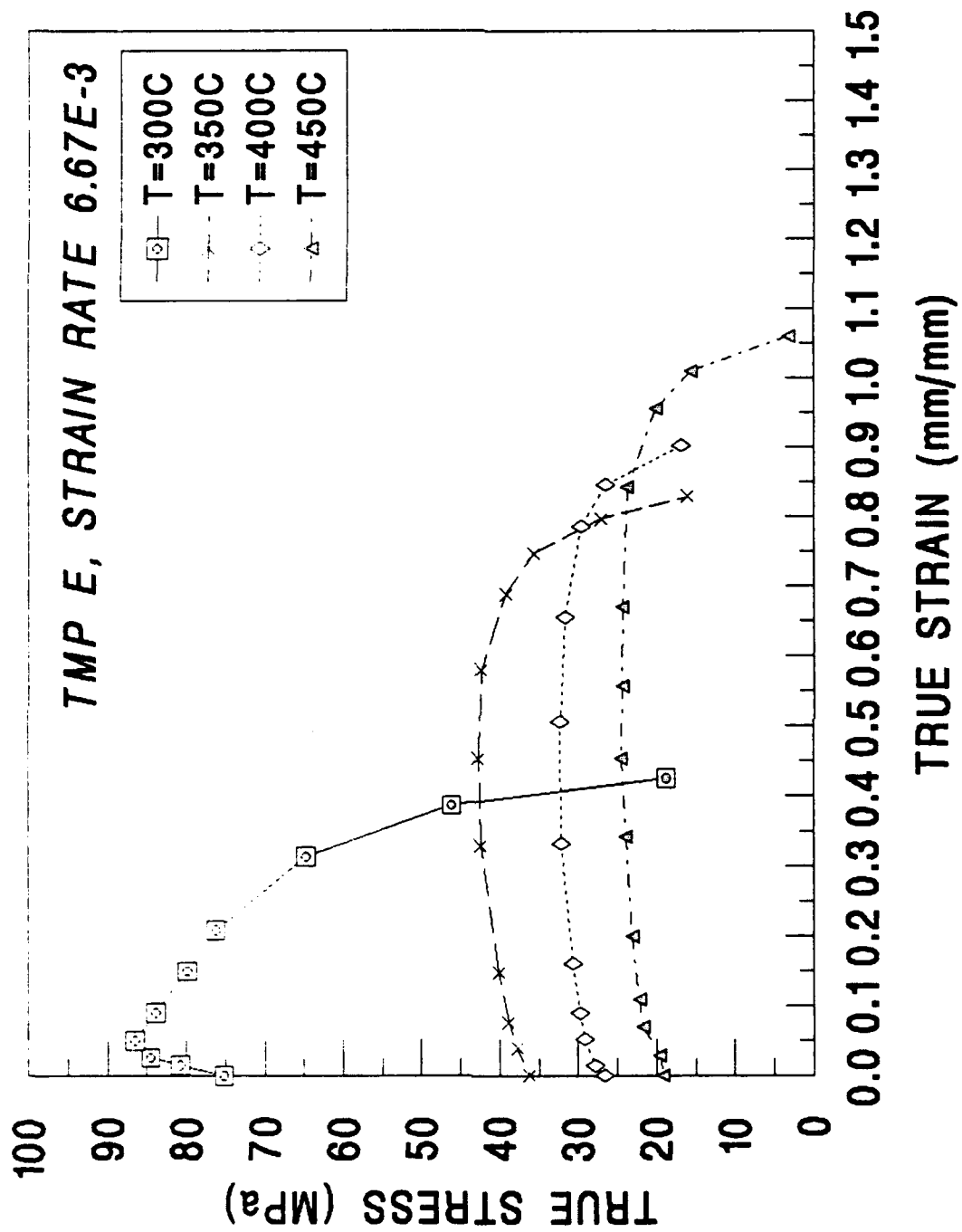
Figure A.9   TMP E, $\dot{\epsilon} = 6.67 \times 10^{-3}$ s^{-1}.

Figure A.10   TMP E, $\dot\epsilon = 6.67 \times 10^{-4}$ s^{-1}.
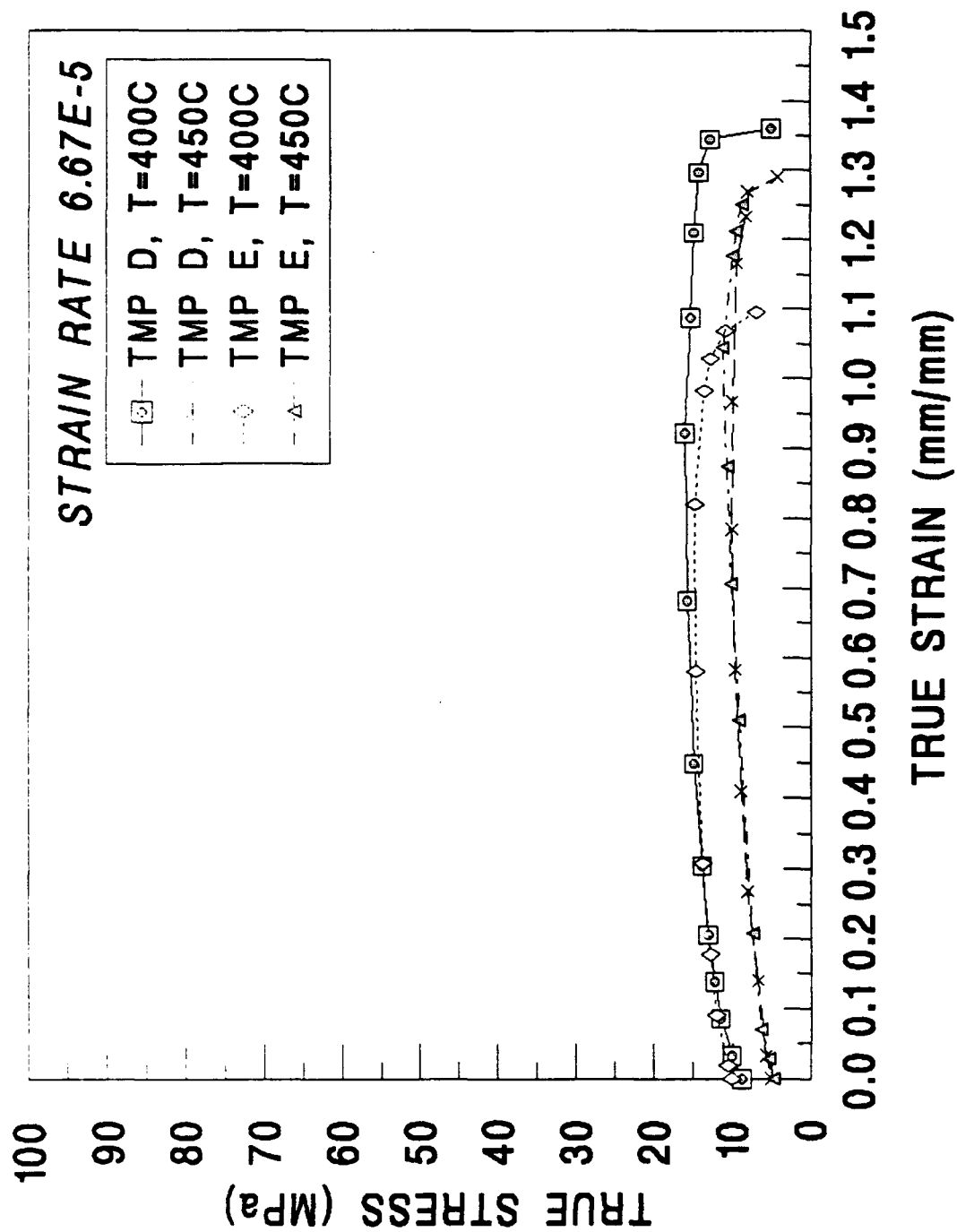
Figure A.11 TMP D AND TMP E, $\dot{\epsilon}=6.67\text{x}10^{-5}$ s^{-1}.
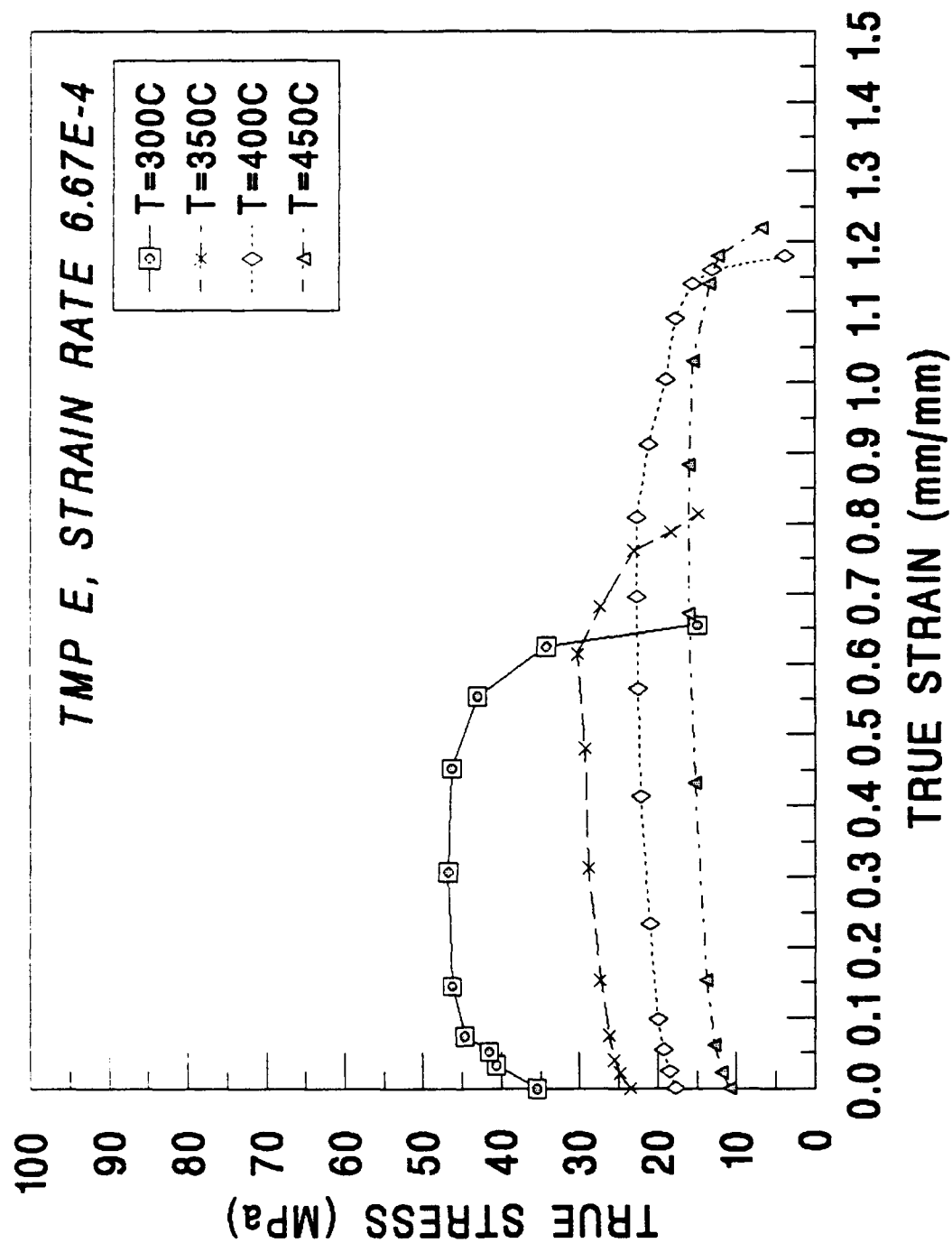
71
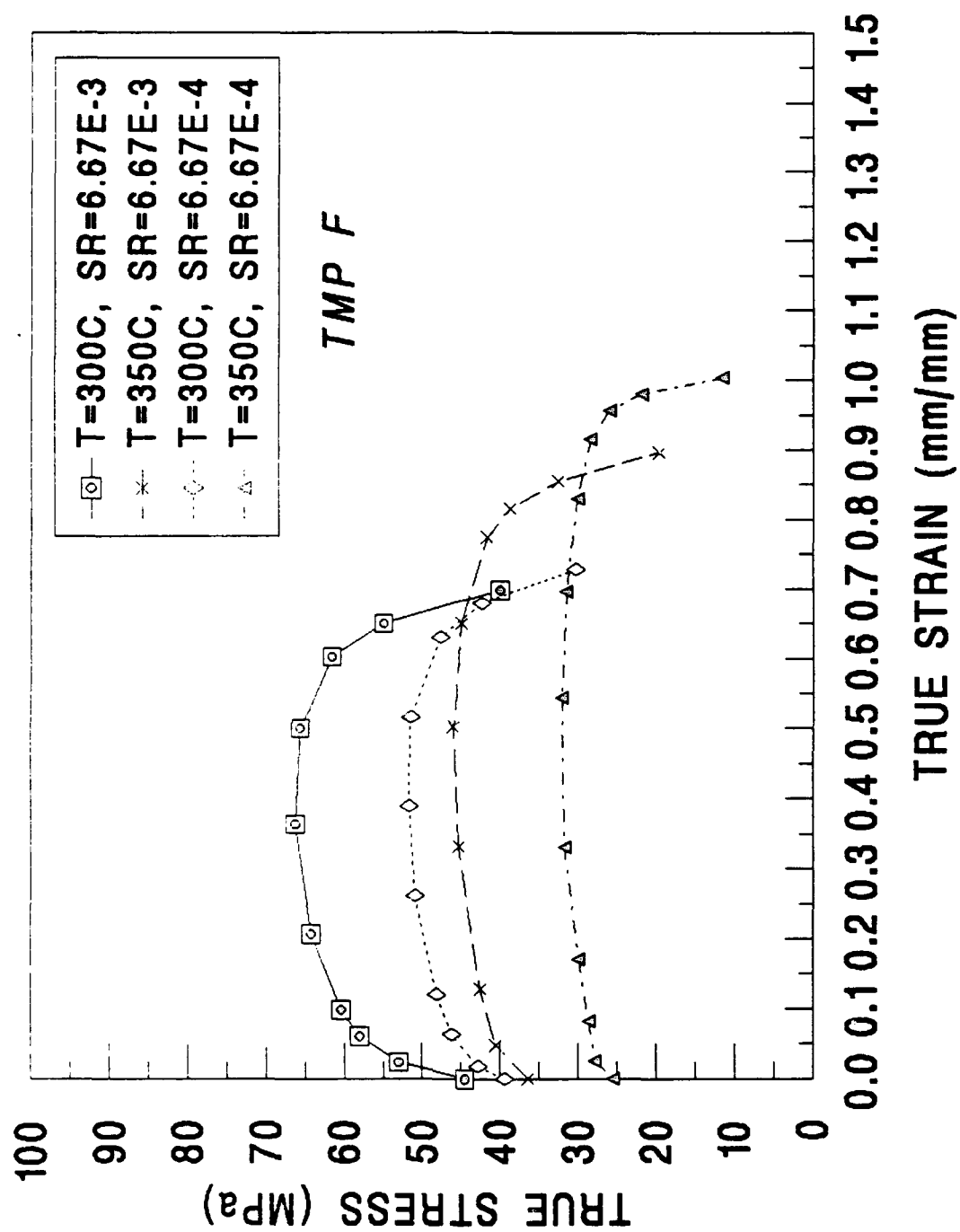
Figure A.12 TMP F, $\dot{\epsilon} = 6.67 \times 10^{-3}$ s^{-1} and 6.67×10^{-4} s^{-1}.
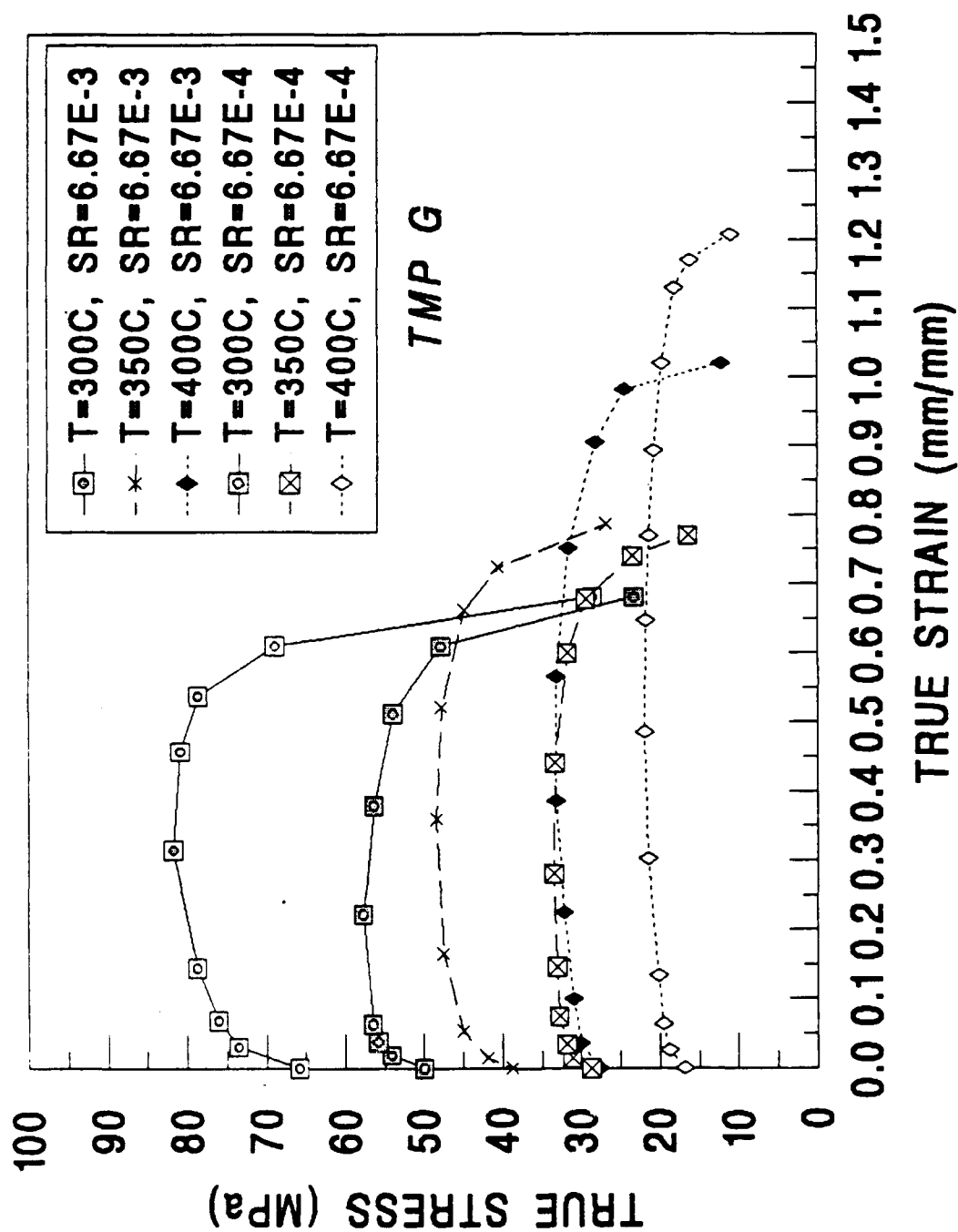
Figure A.13 TMP G, $\dot{\epsilon} = 6.67 \times 10^{-3}$ s^{-1} and 6.67×10^{-4} s^{-1}.

APPENDIX B: STRAIN RATE SENSITIVITY COEFFICIENT (m)

TABLE B.I   STRAIN RATE SENSITIVITY COEFFICIENT (m)

TMP	TEST TEMPERATURE			
	350°C	350°C	400°C	450°C
A	-	.232	.169	.231
B	.188	.183	.207	.134
C	.253	.139	.206	.106
D	.173	.149	.194	.238
E	.263	.165	.176	.229
F	.101	.161	-	-
G	.133	.151	.176	-

APPENDIX C: DUCTILITY DATA SUMMARY

TABLE C.I DUCTILITY DATA

TMP/STRAIN RATE S^{-1}	ELONGATION (PCT)			
	TEST TEMPERATURE (°C)			
	300°C	350°C	400°C	450°C
A/6.67X10^{-3}	78	71	115	142
A/6.67X10^{-4}	93	96	161	164
A/6.67X10^{-5}	-	-	98	152
B/6.67X10^{-3}	66	59	92	140
B/6.67X10^{-4}	112	85	104	206
B/6.67X10^{-5}	-	-	107	-
C/6.67X10^{-3}	41	73	88	131
C/6.67X10^{-4}	69	120	105	133
C/6.67X10^{-5}			114	
D/6.67X10^{-3}	55	104	154	214
D/6.67X10^{-4}	84	107	195	230
D/6.67X10^{-5}	-	-	260	232
E/6.67X10^{-3}	44	119	142	165
E/6.67X10^{-4}	83	114	204	210
E/6.67X10^{-5}			185	215
F/6.67X10^{-3}	94	136	-	-
F/6.67X10^{-4}	98	160	-	-
G/6.67X10^{-3}	89	114	160	-
G/6.67X10^{-4}	94	111	219	-

LIST OF REFERENCES

1. Pilling, J, and Ridley, N., *Superplasticity in Crystalline Solids*, The Institute of Metals, 1989.

2. McNelley, T.R., and Hales, S.J., "Superplastic Aluminum Alloys," *Naval Research Reviews*, Vol. 39.1, pp.51-57, Office of Naval Research, 1987.

3. Product Information, Northrup Corporation, Hawthorne, CA., Nov.,1983.

4. Baudelet, B., "Industrial Aspects of Superplasticity," *Material Science and Engineering*, A137, pp. 41-55, 1991.

5. Watts, B.M., Stowell, M.J., Baikie, B.L., and Owen, D.G.E., "Superplasticity in Al-Cu-Zr Alloys, Part I: Material Preparation and Properties," *Metal Science Journal*, Vol. 10, No. 6, pp. 189-197, June 1976.

6. Wert, J.A., "Grain Refinement and Grain Size Control," *Superplastic Aluminum Alloys,* edited by Paton, N.E., and Hamilton, C.H., pp. 69-83, Conference Proceedings, TMS-AIME, Warrendale, Pa., 1982.

7. Hales, S.J., McNelley, T.R., and McQueen, H.J., "Recrystallization and Superplasticity at 300°C in and Aluminum-Magnesium Alloy," *Metallurgical Transactions A*, Vol. 22A, pp. 1037-1047, May 1991.

8. Crooks, R., Kalu, P.N., and McNelley, T.R., "Use of Backscattered Electron Imaging to Characterize Microstructure of a Superplastic Al-10Mg-0.1Zr Alloy," *Scripta Metallurgica*, Vol. 25, pp. 1321-1325, 1991.

9. *Metals Handbook*, 10ed., Vol. 2, pp. 3-80, American Society for Metals, 1991.

10. Askeland, D.R., *The Science and Engineering of Materials,* The Science and Engineering of Materials, 2nd edition, PWS-Kent Publishing Company, 1989.

11. Meycis, M.A., and Chawla, K.K., *Mechanical Metallurgy Principles and Applications*, Prentice-Hall, Inc., 1984.

12. *Metals Handbook*, 9th ed., Vol. 2, p. 29, American Society for Metals, 1991.

13. "Binary Alloy Phase Diagrams," *American Society for Metals*, Vol. 1, Metals Park, Ohio, 1986.

14. *ASM Handbook*, 10th ed., Vol. 4, pp. 823-880, American Society for Metals, 1991.

15. Mondolfo, L.F., "Aluminum Alloys: Structure and Properties," Butterworths, London, 1976.

16. Crooks, R., Hales, S.J., and McNelley, T.R., "Microstructural Refinement via Continuous Recrystallization in a Superplastic Aluminum Alloy," *Superplasticity and Superplastic Forming*, edited by Hamilton, C.H., and Paton, N.E., pp. 389-393, The Minerals, Metals, & Materials Society, 1988.

17. Watts, B. M., Stowell, M.J., Baikie, B.L., and Owen, D.G.E., "Superplasticity in Al-Cu-Zr Alloys, Part II: Microstructual Study," *Metal Science Journal*, Vol. 10, No. 6, pp. 189-197, 1976.

18. Humphreys, F.J., "Nucleation of Recrystallization in Metals and Alloys with Large Particles," Department of Metallurgy and Materials Science, Imperial College, London, SW7, England.

19. Mathé, W., *Precipitate Coarsening During Overaging of 2519 Al-Cu Alloy: Application to Superplastic Response*, Master's Thesis, Naval Postgraduate School, Monterey, Ca., March 1990.

20. Willig, V., and Heimendahl, M., "Problems of Particle Coarsening Of Disk Shaped Θ Particles in Aluminum Alloy 2219," Institut fur Wefkstoffwissenschaften 1 der Universitat Erlangen-Nurnberg, pp. 674-681.

21. Vietz, J.T., and Polmear, J., Inst. Metals, pp. 94,410, 1966.

INITIAL DISTRIBUTION LIST

No. Copies

1. Defense Technical Information Center   2
   Cameron Station
   Alexandria, Virginia 22304-6145

2. Library, Code 52   2
   Naval Postgraduate School
   Monterey, California 93943-5002

3. Naval Engineering Curricular Office   1
   Code 34
   Naval Postgraduate School
   Monterey, California 93943

4. Professor T.R. McNelley, Code ME/Mc   4
   Department of Mechanical Engineering
   Naval Postgraduate School
   Monterey, California 93943

5. Adjunct Professor P.N. Kalu, Code ME/Mc   1
   Department of Mechanical Engineering
   Naval Postgraduate School
   Monterey, California 93943

6. Adjunct Professor R. Crooks, Code ME/Mc   1
   Department of Mechanical Engineering
   Naval Postgraduate School
   Monterey, California 93943

7. Dr. Lewis Sloter, Code AIR 913A   1
   Headquarters, Naval Air Systems Command
   Washington, D.C. 20361

8. LT Scott Bohman   1
   5840 County Trunk O
   Rudolph, Wisconsin 54475